Points of quantum SL_n coming from quantum snakes

DANIEL C DOUGLAS

Points of quantum SL$_n$ coming from quantum snakes

DANIEL C DOUGLAS

We show that the quantized Fock–Goncharov monodromy matrices satisfy the relations of the quantum special linear group SL$_n^q$. The proof employs a quantum version of the technology of Fock and Goncharov, called snakes. This relationship between higher Teichmüller theory and quantum group theory is integral to the construction of an SL$_n$–quantum trace map for knots in thickened surfaces, partially developed in previous work of the author.

Introduction

For a finitely generated group Γ and a suitable Lie group G, a primary object of study in low-dimensional geometry and topology is the G–character variety

$$\mathcal{R}_G(\Gamma) = \{\rho \colon \Gamma \to G\} \mathbin{/\mkern-5mu/} G$$

consisting of group homomorphisms ρ from Γ to G, considered up to conjugation. Here the quotient is taken in the algebraic geometric sense of geometric invariant theory; see Mumford, Fogarty, and Kirwan [25]. Character varieties can be explored using a wide variety of mathematical skill sets. Some examples include the Higgs bundle approach of Hitchin [18], the dynamics approach of Labourie [23], and the representation theory approach of Fock and Goncharov [9].

In the case where the group $\Gamma = \pi_1(\mathfrak{S})$ is the fundamental group of a punctured surface $\mathfrak{S}$ of finite topological type, and where the Lie group $G = \mathrm{SL}_n(\mathbb{C})$ is the special linear group, we are interested in studying a relationship between two competing deformation quantizations of the character variety $\mathcal{R}_{\mathrm{SL}_n(\mathbb{C})}(\mathfrak{S}) := \mathcal{R}_{\mathrm{SL}_n(\mathbb{C})}(\pi_1(\mathfrak{S}))$. Here a deformation quantization $\{\mathcal{R}^q\}_q$ of a Poisson space $\mathcal{R}$ is a family of noncommutative algebras $\mathcal{R}^q$ parametrized by a nonzero complex parameter $q = e^{2\pi i \hbar}$, such that the lack of commutativity in $\mathcal{R}^q$ is infinitesimally measured in the classical limit $\hbar \to 0$ by the Poisson bracket of the space $\mathcal{R}$. In the case where $\mathcal{R} = \mathcal{R}_{\mathrm{SL}_n(\mathbb{C})}(\mathfrak{S})$ is the character variety, the bracket is provided by the Goldman Poisson structure on $\mathcal{R}_{\mathrm{SL}_n(\mathbb{C})}(\mathfrak{S})$ [15; 16].

The first quantization of the character variety is the $\mathrm{SL}_n(\mathbb{C})$–skein algebra $\mathcal{S}_n^q(\mathfrak{S})$ of the surface $\mathfrak{S}$; see Bullock, Frohman, and Kania-Bartoszyńska [3], Kuperberg [22], Przytycki [27], Sikora [30], Turaev [32], and Witten [33]. The skein algebra is motivated by the classical algebraic geometric approach to studying the character variety $\mathcal{R}_{\mathrm{SL}_n(\mathbb{C})}(\mathfrak{S})$ via its algebra of regular functions $\mathbb{C}[\mathcal{R}_{\mathrm{SL}_n(\mathbb{C})}(\mathfrak{S})]$. An example of

a regular function is the trace function $\mathrm{Tr}_\gamma \colon \mathcal{R}_{\mathrm{SL}_n(\mathbb{C})}(\mathfrak{S}) \to \mathbb{C}$ associated to a closed curve $\gamma \in \pi_1(\mathfrak{S})$ sending a representation $\rho \colon \pi_1(\mathfrak{S}) \to \mathrm{SL}_n(\mathbb{C})$ to the trace $\mathrm{Tr}(\rho(\gamma)) \in \mathbb{C}$ of the matrix $\rho(\gamma) \in \mathrm{SL}_n(\mathbb{C})$. A theorem of classical invariant theory, due to Procesi [26], implies that the trace functions Tr_γ generate the algebra of functions $\mathbb{C}[\mathcal{R}_{\mathrm{SL}_n(\mathbb{C})}(\mathfrak{S})]$ as an algebra. According to the philosophy of Turaev and Witten, quantizations of the character variety should be of a 3–dimensional nature. Indeed, knots (or links) K in the thickened surface $\mathfrak{S} \times (0, 1)$ represent elements of the skein algebra $\mathcal{S}_n^q(\mathfrak{S})$. The skein algebra $\mathcal{S}_n^q(\mathfrak{S})$ has the advantage of being natural, but can be difficult to study directly.

The second quantization of the $\mathrm{SL}_n(\mathbb{C})$–character variety is the Fock–Goncharov quantum space $\mathcal{T}_n^q(\mathfrak{S})$; see Fock and Goncharov [12], Fock and Chekhov [7], and Kashaev [20]. At the classical level, Fock and Goncharov [9] introduced a framed version $\mathcal{R}_{\mathrm{PSL}_n(\mathbb{C})}(\mathfrak{S})_{\mathrm{fr}}$ (called the $\mathcal{X}$–space) of the $\mathrm{PSL}_n(\mathbb{C})$–character variety, which, roughly speaking, consists of representations $\rho \colon \pi_1(\mathfrak{S}) \to \mathrm{PSL}_n(\mathbb{C})$ equipped with additional linear algebraic data attached to the punctures of $\mathfrak{S}$. Associated to each ideal triangulation λ of the punctured surface $\mathfrak{S}$ is a λ–coordinate chart U_λ for $\mathcal{R}_{\mathrm{PSL}_n(\mathbb{C})}(\mathfrak{S})_{\mathrm{fr}}$ parametrized by N nonzero complex coordinates $X_1, X_2, \ldots, X_N$ where the integer N depends only on the topology of the surface $\mathfrak{S}$ and the rank of the Lie group $\mathrm{SL}_n(\mathbb{C})$. These coordinates X_i are computed by taking various generalized cross-ratios of configurations of n–dimensional flags attached to the punctures of $\mathfrak{S}$. When written in terms of these coordinates X_i, the trace functions $\mathrm{Tr}_\gamma = \mathrm{Tr}_\gamma(X_i^{\pm 1/n})$ associated to closed curves γ take the form of Laurent polynomials in n–roots of the variables X_i. At the quantum level, there are q–deformed versions X_i^q of these coordinates, which no longer commute but q–commute with each other. The quantized character variety $\mathcal{T}_n^q(\mathfrak{S})$ is obtained by gluing together quantum tori $\mathcal{T}_n^q(\sigma)$, including one for each triangulation $\sigma = \lambda$ consisting of Laurent polynomials in the quantized Fock–Goncharov coordinates X_i^q. The quantum character variety $\mathcal{T}_n^q(\mathfrak{S})$ has the advantage of being easier to work with than the skein algebra $\mathcal{S}_n^q(\mathfrak{S})$, however it is less intrinsic.

We are interested in studying q–deformed versions Tr_γ^q of the trace functions Tr_γ, associating to a closed curve γ a Laurent polynomial in the quantized Fock–Goncharov coordinates X_i^q. Turaev and Witten's philosophy leads us from the 2–dimensional setting of curves γ on the surface $\mathfrak{S}$ to the 3–dimensional setting of knots K in the thickened surface $\mathfrak{S} \times (0, 1)$. In the case of $\mathrm{SL}_2(\mathbb{C})$, such a *quantum trace map* was developed by Bonahon and Wong [1] as an injective algebra homomorphism

$$\mathrm{Tr}^q(\lambda) \colon \mathcal{S}_2^q(\mathfrak{S}) \hookrightarrow \mathcal{T}_2^q(\lambda)$$

from the $\mathrm{SL}_2(\mathbb{C})$–skein algebra to (the λ–quantum torus of) the quantized $\mathrm{SL}_2(\mathbb{C})$–character variety. Their construction is "by hand", but is implicitly related to the theory of the quantum group $\mathrm{U}_q(\mathfrak{sl}_2)$ or, more precisely, of its Hopf dual SL_2^q; see Kassel [21]. Developing a quantum trace map for $\mathrm{SL}_n(\mathbb{C})$ requires a more conceptual approach, making explicit this connection between higher Teichmüller theory and quantum group theory. In a companion paper [6], we make significant progress in this direction. Our goal here is to establish a local building block result that is essential to understanding the quantum trace map more conceptually.

Whereas the classical trace $\text{Tr}_\gamma(\rho) \in \mathbb{C}$ is a number obtained by evaluating the trace of an SL$_n(\mathbb{C})$–monodromy $\rho(\gamma)$ taken along a curve γ in the surface $\mathfrak{S}$, the quantum trace $\text{Tr}_K(X_i^q) \in \mathcal{T}_n^q(\lambda)$ is a Laurent polynomial obtained from a quantum monodromy associated to a knot K in the thickened surface $\mathfrak{S} \times (0,1)$. This quantum monodromy is essentially constructed by chopping the knot K into little pieces, namely the components C of $K \cap (\lambda_k \times (0,1))$ where the λ_k are the triangles of the ideal triangulation λ, and associating to each piece C a local quantum monodromy matrix $M_C^q \in \text{M}_n(\mathcal{T}_n^q(\lambda_k))$. Here the coefficients of the matrix M_C^q lie in a local quantum torus $\mathcal{T}_n^q(\lambda_k)$ associated to the triangle λ_k, closely associated to the quantum torus $\mathcal{T}_n^q(\lambda)$.

Theorem *When C is an arc on the corner of a triangle λ_k, the Fock–Goncharov quantum matrix $M_C^q \in \text{M}_n(\mathcal{T}_n^q(\lambda_k))$ is a $\mathcal{T}_n^q(\lambda_k)$–point of the quantum special linear group SL_n^q. In other words, each such matrix defines an algebra homomorphism*

$$\varphi(M_C^q) \colon \text{SL}_n^q \to \mathcal{T}_n^q(\lambda_k)$$

by the property that the n^2–many generators of the algebra SL_n^q are sent to the corresponding n^2–many entries of the matrix M_C^q (see Section 2.4.1).

See Theorem 2.8 (and Douglas [5, Theorem 3.10]). Our proof uses a quantum version of the technology of Fock and Goncharov, called snakes.

The main property of the quantum trace $\text{Tr}_K(X_i^q) \in \mathcal{T}_n^q(\lambda)$ is its invariance under isotopy of the knot K. This is equivalent to invariance under a handful of local Reidemeister-like moves in the thickened triangulated surface. These topological moves are independent of n, and can be seen as the oriented versions of the moves depicted in [1, Figures 15–19]. In particular, due to their local nature, these moves have a purely algebraic formulation as equalities involving $n \times n$ matrices with coefficients in the quantum torus. Our main result is essentially equivalent to the algebraic formulation of one of these moves, specifically that depicted in [1, Figure 17]; see also [6, Section 6].

For an independent study of these same algebraic identities underlying the isotopy invariance of the quantum trace map, in the context of integrable systems, see Chekhov and Shapiro [4, Theorems 2.12 and 2.14] (which, in particular, reproduces our main result). This was motivated in part by Schrader and Shapiro [28; 29]; see also Fock and Goncharov [8], Gekhtman, Shapiro, and Vainshtein [14], and Goncharov and Shen [17]. Our work complements that of [4] by focusing attention on a single isotopy move, and conceptualizing the associated quantum phenomenon as arising naturally from the underlying geometry.

Acknowledgements

1 Fock–Goncharov snakes

We recall some of the classical (as opposed to the quantum) geometric theory of Fock and Goncharov [9], underlying the quantum theory discussed later on; see also [10; 11]. This section is a condensed version of [5, Chapter 2]. For other references on Fock–Goncharov coordinates and snakes see [19; 13; 24]. When $n = 2$, these coordinates date back to Thurston's shearing coordinates for Teichmüller space [31].

Let $n \in \mathbb{Z}$ for $n \geqslant 2$, and $V = \mathbb{C}^n$ be the standard n–dimensional complex vector space.

1.1 Generic configurations of flags and Fock–Goncharov invariants

A (*complete*) *flag* E in V is a collection of linear subspaces $E^{(a)} \subseteq V$ indexed by $0 \leqslant a \leqslant n$, satisfying the property that each subspace $E^{(a)}$ is properly contained in the subspace $E^{(a+1)}$. In particular, $E^{(a)}$ is a–dimensional, $E^{(0)} = \{0\}$, and $E^{(n)} = V$. Denote the space of flags by $\mathrm{Flag}(V)$.

1.1.1 Generic triples and quadruples of flags There are at least two notions of genericity for a configuration of flags. We will use just one of them, the maximum span property; for a complementary notion, the minimum intersection property see [5, Section 2.10].

Definition 1.1 A flag tuple $(E_1, E_2, \ldots, E_k) \in \mathrm{Flag}(V)^k$ satisfies the *maximum span property* if either of the following equivalent conditions are satisfied: for all $0 \leqslant a_1, a_2, \ldots, a_k \leqslant n$,

(1) for all $a_1 + a_2 + \cdots + a_k = n$, the sum $E_1^{(a_1)} + E_2^{(a_2)} + \cdots + E_k^{(a_k)} = E_1^{(a_1)} \oplus E_2^{(a_2)} \oplus \cdots \oplus E_k^{(a_k)}$ is direct, and thus the sum is V, or

(2) the dimension formula $\dim(E_1^{(a_1)} + E_2^{(a_2)} + \cdots + E_k^{(a_k)})$ equals $\min(a_1 + a_2 + \cdots + a_k, n)$.

In the case $n = 3$, such a flag triple $(E, F, G) \in \mathrm{Flag}(V)^3$ is called a *maximum span flag triple*, and in the case $n = 4$, such a flag quadruple $(E, F, G, H) \in \mathrm{Flag}(V)^4$ is called a *maximum span flag quadruple*.

1.1.2 Discrete triangle The *discrete n–triangle* $\Theta_n \subseteq \mathbb{Z}_{\geqslant 0}^3$ is defined by

$$\Theta_n = \{(a, b, c) \in \mathbb{Z}_{\geqslant 0}^3 \mid a + b + c = n\}.$$

See Figure 1. The *interior* $\mathrm{int}(\Theta_n) \subseteq \Theta_n$ of the discrete triangle is defined by

$$\mathrm{int}(\Theta_n) = \{(a, b, c) \in \Theta_n \mid a, b, c > 0\}.$$

An element $v \in \Theta_n$ is called a *vertex* of Θ_n. Put $\Gamma(\Theta_n) = \{(n, 0, 0), (0, n, 0), (0, 0, n)\} \subseteq \Theta_n$. An element $v \in \Gamma(\Theta_n)$ is called a *corner vertex* of Θ_n.

1.1.3 Fock–Goncharov triangle and edge invariants For a maximum span triple of flags $(E, F, G) \in \mathrm{Flag}(V)^3$, Fock and Goncharov assigned to each interior point $(a, b, c) \in \mathrm{int}(\Theta_n)$ a *triangle invariant* $\tau_{abc}(E, F, G) \in \mathbb{C} - \{0\}$, defined by the formula

$$\tau_{abc}(E, F, G) = \frac{e^{(a-1)} \wedge f^{(b+1)} \wedge g^{(c)}}{e^{(a+1)} \wedge f^{(b-1)} \wedge g^{(c)}} \frac{e^{(a)} \wedge f^{(b-1)} \wedge g^{(c+1)}}{e^{(a)} \wedge f^{(b+1)} \wedge g^{(c-1)}} \frac{e^{(a+1)} \wedge f^{(b)} \wedge g^{(c-1)}}{e^{(a-1)} \wedge f^{(b)} \wedge g^{(c+1)}} \in \mathbb{C} - \{0\}.$$
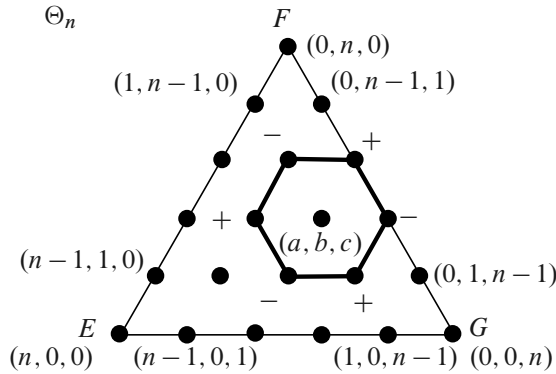
Figure 1: Discrete triangle, and triangle invariants for a generic flag triple.

Here $e^{(a')}$, $f^{(b')}$, and $g^{(c')}$ are choices of generators for the exterior powers $\Lambda^{a'}(E^{(a')}) \subseteq \Lambda^{a'}(V)$, $\Lambda^{b'}(F^{(b')}) \subseteq \Lambda^{b'}(V)$, and $\Lambda^{c'}(G^{(c')}) \subseteq \Lambda^{c'}(V)$, respectively. The maximum span property ensures that each wedge product $e^{(a')} \wedge f^{(b')} \wedge g^{(c')}$ is nonzero in $\Lambda^{a'+b'+c'}(V) = \Lambda^n(V) \cong \mathbb{C}$. Since there are the same number of terms in the numerator as the denominator, $\tau_{abc}(E, F, G)$ is independent of this choice of isomorphism $\Lambda^n(V) \cong \mathbb{C}$. Since each generator $e^{(a')}$, $f^{(b')}$, and $g^{(c')}$ appears exactly once in the numerator and denominator, $\tau_{abc}(E, F, G)$ is independent of the choices of these generators.

The six numerators and denominators appearing in the expression defining $\tau_{abc}(E, F, G)$ can be visualized as the vertices of a hexagon in Θ_n centered at (a, b, c); see Figure 1.

Similarly, for a maximum span quadruple of flags $(E, G, F, F') \in \mathrm{Flag}(V)^4$, Fock and Goncharov assigned to each integer $1 \leqslant j \leqslant n - 1$ an *edge invariant* $\epsilon_j(E, G, F, F')$ by

$$\epsilon_j(E, G, F, F') = -\frac{e^{(j)} \wedge g^{(n-j-1)} \wedge f^{(1)}}{e^{(j)} \wedge g^{(n-j-1)} \wedge f'^{(1)}} \frac{e^{(j-1)} \wedge g^{(n-j)} \wedge f'^{(1)}}{e^{(j-1)} \wedge g^{(n-j)} \wedge f^{(1)}} \in \mathbb{C} - \{0\}.$$

The four numerators and denominators appearing in the expression defining $\epsilon_j(E, G, F, F')$ can be visualized as the vertices of a square, which crosses the "common edge" between two "adjacent" discrete triangles $\Theta_n(G, F, E)$ and $\Theta_n(E, F', G)$; see Figure 2.
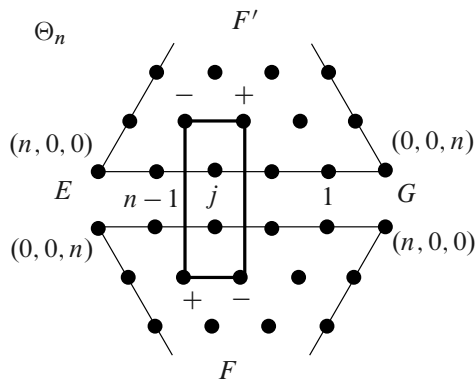
Figure 2: Edge invariants for a generic flag quadruple.

1.1.4 Action of PGL(V) on generic flag triples The action of the general linear group GL(V) on the vector space V induces an action of the projective linear group PGL(V) on the space Flag(V) of flags. The corresponding diagonal action of PGL(V) on Flag(V)^n restricts to generic configurations of flags. By an elementary argument, for $n = 2$ this diagonal action on generic flag pairs (E, F) has a single orbit in Flag(V)^2.

Theorem 1.2 (Fock and Goncharov) *Two maximum span flag triples (E, F, G) and (E', F', G') have the same triangle invariants, namely $\tau_{abc}(E, F, G) = \tau_{abc}(E', F', G') \in \mathbb{C} - \{0\}$ for every $(a, b, c) \in \mathrm{int}(\Theta_n)$, if and only if there exists $\varphi \in \mathrm{PGL}(V)$ such that $(\varphi E, \varphi F, \varphi G) = (E', F', G') \in \mathrm{Flag}(V)^3$.*

Conversely, for each choice of nonzero complex numbers $x_{abc} \in \mathbb{C} - \{0\}$ assigned to the interior points $(a, b, c) \in \mathrm{int}(\Theta_n)$, there exists a maximum span flag triple (E, F, G) such that $\tau_{abc}(E, F, G) = x_{abc}$ for all (a, b, c).

Proof See [9, Section 9]. The proof uses the concept of snakes, due to Fock and Goncharov. For a sketch of the proof and some examples see [5, Section 2.19]. ☐

1.2 Snakes and projective bases

1.2.1 Snakes Snakes are combinatorial objects associated to the $(n-1)$–discrete triangle Θ_{n-1}; see Section 1.1.2. In contrast to Θ_n, we denote the coordinates of a vertex $\nu \in \Theta_{n-1}$ by $\nu = (\alpha, \beta, \gamma)$ corresponding to solutions $\alpha + \beta + \gamma = n - 1$ for $\alpha, \beta, \gamma \in \mathbb{Z}_{\geq 0}$.

Definition 1.3 A *snake-head* η is a fixed corner vertex of the $(n-1)$–discrete triangle

$$\eta \in \{(n - 1, 0, 0), (0, n - 1, 0), (0, 0, n - 1)\} = \Gamma(\Theta_{n-1}) \subseteq \Theta_{n-1}.$$

Remark 1.4 In a moment, we will define a snake. The most general definition involves choosing a snake-head $\eta \in \Gamma(\Theta_{n-1})$. For simplicity, we define a snake only in the case $\eta = (n - 1, 0, 0)$. The definition for other choices of snake-heads follows by triangular symmetry. We will usually take $\eta = (n - 1, 0, 0)$ and will alert the reader if otherwise.

Definition 1.5 A *left n–snake* (for the snake-head $\eta = (n - 1, 0, 0) \in \Gamma(\Theta_{n-1})$), or just *snake*, σ is an ordered list $\sigma = (\sigma_1, \sigma_2, \ldots, \sigma_n) \in (\Theta_{n-1})^n$ of n–many vertices $\sigma_k = (\alpha_k, \beta_k, \gamma_k)$ in the discrete triangle Θ_{n-1}, called *snake-vertices*, satisfying

$$\alpha_k = k - 1, \quad \beta_k \geq \beta_{k+1}, \quad \text{and} \quad \gamma_k \geq \gamma_{k+1} \quad \text{for } k = 1, 2, \ldots, n.$$

See Figure 3. On the right-hand side, we show a snake $\sigma = (\sigma_k)_k$ in the case $n = 5$ (where we have taken some artistic license to assist the reader in locating the snake's head and tail; in Section 3, we will find it useful to split the snake in half down its length, as illustrated in Figure 15). On the left-hand side, we show how the snake-vertices $\sigma_k \in \Theta_{n-1}$ can be pictured as small upward-facing triangles Δ in the n–discrete triangle Θ_n.
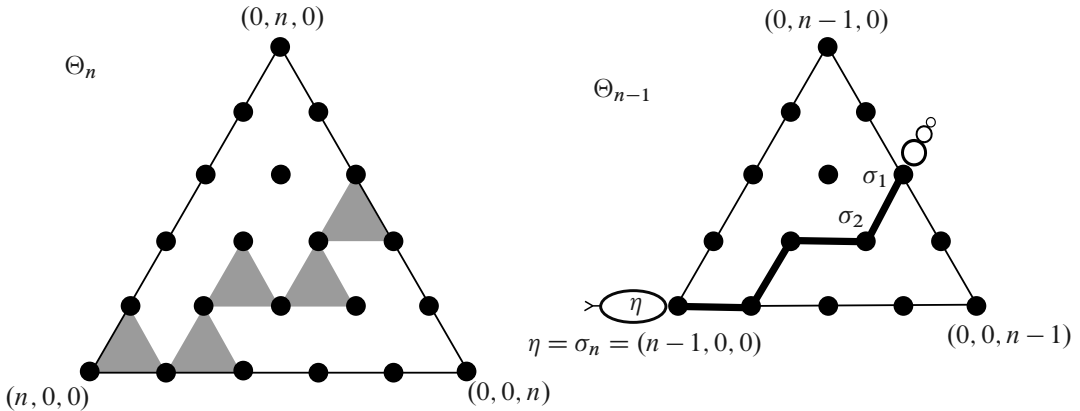
Figure 3: Snake.

1.2.2 Line decomposition of V^* associated to a generic triple of flags and a snake

Let $V^* = \{$linear map $V \to \mathbb{C}\}$. For a subspace $W \subseteq V$, define $W^\perp = \{u \in V^* \mid u(w) = 0 \text{ for all } w \in W\}$. A *line* in a vector space V' is a 1–dimensional subspace.

Fix a maximum span triple $(E, F, G) \in \text{Flag}(V)^3$. For any vertex $v = (\alpha, \beta, \gamma) \in \Theta_{n-1}$,

$$\dim((E^{(\alpha)} \oplus F^{(\beta)} \oplus G^{(\gamma)})^\perp) = 1$$

by the maximum span property, since $\alpha + \beta + \gamma = n - 1$. Consequently, the subspace

$$L_{(\alpha,\beta,\gamma)} := (E^{(\alpha)} \oplus F^{(\beta)} \oplus G^{(\gamma)})^\perp \subseteq V^*$$

is a line for all vertices $(\alpha, \beta, \gamma) \in \Theta_{n-1}$.

If in addition we are given a snake $\sigma = (\sigma_k)_k$, then we may consider the n–many lines

$$L_{\sigma_k} = L_{(\alpha_k, \beta_k, \gamma_k)} \subseteq V^* \quad \text{for } k = 1, \dots, n,$$

where $\sigma_k = (\alpha_k, \beta_k, \gamma_k) \in \Theta_{n-1}$. By genericity, we obtain a direct sum line decomposition

$$V^* = \bigoplus_{k=1}^{n} L_{\sigma_k}.$$

1.2.3 Projective basis of V^* associated to a generic triple of flags and a snake

Given a generic flag triple (E, F, G) and a snake σ, Fock and Goncharov construct in addition a projective basis $[\mathcal{U}]$ of V^* adapted to the associated line decomposition. Here $\mathcal{U} = \{u_1, u_2, \dots, u_n\}$ is a linear basis of V^* such that $u_k \in L_{\sigma_k}$ for all k, and the *projective basis* $[\mathcal{U}]$ is the equivalence class of $\mathcal{U}$ under the relation $\{u_1, u_2, \dots, u_n\} \sim \{\lambda u_1, \lambda u_2, \dots, \lambda u_n\}$ for all $\lambda \neq 0$.

Put $\sigma_k = (\alpha_k, \beta_k, \gamma_k)$. We begin by choosing a covector u_n in the line $L_{\sigma_n} \subseteq V^*$, called a *normalization*. Having defined covectors $u_n, u_{n-1}, \dots, u_{k+1}$, we will define a covector

$$u_k \in L_{\sigma_k} = (E^{(\alpha_k)} \oplus F^{(\beta_k)} \oplus G^{(\gamma_k)})^\perp \subseteq V^*.$$
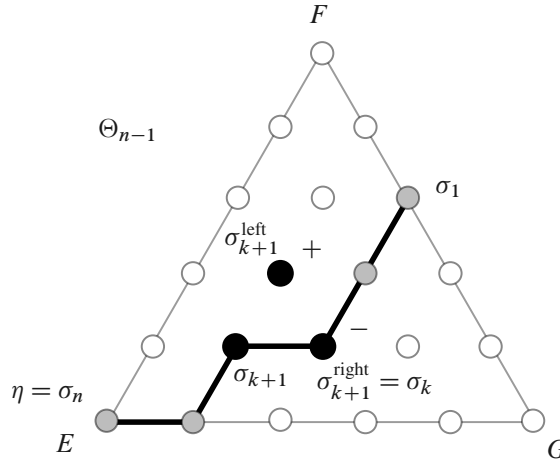
Figure 4: Three coplanar lines involved in the definition of a projective basis. For the meaning of the $+$ and $-$ signs see Definition 1.6.

By the definition of snakes, we see that given σ_{k+1} there are only two possibilities for σ_k, denoted by $\sigma_{k+1}^{\text{left}}$ and $\sigma_{k+1}^{\text{right}}$:

$$\sigma_{k+1}^{\text{left}} = (\alpha_{k+1}^{\text{left}}, \beta_{k+1}^{\text{left}}, \gamma_{k+1}^{\text{left}}) \quad \text{for} \quad \alpha_{k+1}^{\text{left}} = k-1, \quad \beta_{k+1}^{\text{left}} = \beta_{k+1}+1, \quad \gamma_{k+1}^{\text{left}} = \gamma_{k+1},$$

$$\sigma_{k+1}^{\text{right}} = (\alpha_{k+1}^{\text{right}}, \beta_{k+1}^{\text{right}}, \gamma_{k+1}^{\text{right}}) \quad \text{for} \quad \alpha_{k+1}^{\text{right}} = k-1, \quad \beta_{k+1}^{\text{right}} = \beta_{k+1}, \quad \gamma_{k+1}^{\text{right}} = \gamma_{k+1}+1.$$

See Figure 4, in which $\sigma_k = \sigma_{k+1}^{\text{right}}$. Thus the lines $L_{\sigma_{k+1}^{\text{left}}}$ and $L_{\sigma_{k+1}^{\text{right}}}$ can be written

$$L_{\sigma_{k+1}^{\text{left}}} = (E^{(k-1)} \oplus F^{(\beta_{k+1}+1)} \oplus G^{(\gamma_{k+1})})^{\perp} \subseteq V^*,$$

$$L_{\sigma_{k+1}^{\text{right}}} = (E^{(k-1)} \oplus F^{(\beta_{k+1})} \oplus G^{(\gamma_{k+1}+1)})^{\perp} \subseteq V^*.$$

It follows by the maximum span property that the three lines $L_{\sigma_{k+1}}$, $L_{\sigma_{k+1}^{\text{left}}}$, and $L_{\sigma_{k+1}^{\text{right}}}$ in V^* are distinct and coplanar. Specifically, they lie in the plane

$$(E^{(k-1)} \oplus F^{(\beta_{k+1})} \oplus G^{(\gamma_{k+1})})^{\perp} \subseteq V^*,$$

which is indeed 2–dimensional, since $(k-1) + \beta_{k+1} + \gamma_{k+1} = (n-1)-1$, as $\alpha_{k+1} = k$. Thus, if u_{k+1} is a nonzero covector in the line $L_{\sigma_{k+1}}$, then there exist unique nonzero covectors u_{k+1}^{left} and u_{k+1}^{right} in the lines $L_{\sigma_{k+1}^{\text{left}}}$ and $L_{\sigma_{k+1}^{\text{right}}}$, respectively, such that

$$u_{k+1} + u_{k+1}^{\text{left}} + u_{k+1}^{\text{right}} = 0 \in V^*.$$

Definition 1.6 Having chosen a normalization $u_n \in L_{\sigma_n} = L_{(n-1,0,0)}$ and having inductively defined $u_{k'} \in L_{\sigma_{k'}}$ for $k' = n, n-1, \ldots, k+1$, define $u_k \in L_{\sigma_k}$ by

(1) $u_k = +u_{k+1}^{\text{left}} \in L_{\sigma_{k+1}^{\text{left}}}$ if $\sigma_k = \sigma_{k+1}^{\text{left}}$,

(2) $u_k = -u_{k+1}^{\text{right}} \in L_{\sigma_{k+1}^{\text{right}}}$ if $\sigma_k = \sigma_{k+1}^{\text{right}}$.

See Figure 4, which falls into (2). Note if the initial normalization u_n is replaced by λu_n for some scalar $\lambda \neq 0$, then u_k is replaced by λu_k for all $1 \leqslant k \leqslant n$. Thus this process produces a projective basis $[\mathcal{U}] = [\{u_1, u_2, \ldots, u_n\}]$ of V^*, as desired. We call $\mathcal{U} = \{u_1, u_2, \ldots, u_n\}$ the *normalized projective basis* for V^* depending on the normalization $u_n \in L_{\sigma_n}$.

1.3 Snake moves

1.3.1 Elementary matrices Let $\mathcal{A}$ be a commutative algebra with 1, such as $\mathcal{A} = \mathbb{C}$. Let $X^{1/n}, Z^{1/n} \in \mathcal{A}$, and put $X = (X^{1/n})^n$ and $Z = (Z^{1/n})^n$. Let $\mathrm{M}_n(\mathcal{A})$ (resp. $\mathrm{SL}_n(\mathcal{A})$) denote the ring of $n \times n$ matrices (resp. having determinant equal to 1) over $\mathcal{A}$ (see also Section 2.1.2).

For $k = 1, 2, \ldots, n-1$ define the kth *left-elementary matrix* $S_k^{\mathrm{left}}(X) \in \mathrm{SL}_n(\mathcal{A})$ by

$$
S_k^{\mathrm{left}}(X) = X^{-(k-1)/n}
\begin{pmatrix}
X & & & & & & & \\
 & \ddots & & & & & & \\
 & & X & & & & & \\
 & & & 1 & 1 & & & \\
 & & & & 1 & & & \\
 & & & & & 1 & & \\
 & & & & & & \ddots & \\
 & & & & & & & 1
\end{pmatrix}
\in \mathrm{SL}_n(\mathcal{A}) \quad \text{where } X \text{ appears } k-1 \text{ times,}
$$

and define the kth *right-elementary matrix* $S_k^{\mathrm{right}}(X) \in \mathrm{SL}_n(\mathcal{A})$ by

$$
S_k^{\mathrm{right}}(X) = X^{+(k-1)/n}
\begin{pmatrix}
1 & & & & & & & \\
 & \ddots & & & & & & \\
 & & 1 & & & & & \\
 & & & 1 & & & & \\
 & & & 1 & 1 & & & \\
 & & & & & X^{-1} & & \\
 & & & & & & \ddots & \\
 & & & & & & & X^{-1}
\end{pmatrix}
\in \mathrm{SL}_n(\mathcal{A}) \quad \text{where } X \text{ appears } k-1 \text{ times.}
$$

Note that $S_1^{\mathrm{left}}(X)$ and $S_1^{\mathrm{right}}(X)$ do not, in fact, involve the variable X, and so we will denote these matrices simply by S_1^{left} and S_1^{right}, respectively.

For $j = 1, 2, \ldots, n-1$ define the jth *edge-elementary matrix* $S_j^{\mathrm{edge}}(Z) \in \mathrm{SL}_n(\mathcal{A})$ by

$$
S_j^{\mathrm{edge}}(Z) = Z^{-j/n}
\begin{pmatrix}
Z & & & & & \\
 & \ddots & & & & \\
 & & Z & & & \\
 & & & 1 & & \\
 & & & & \ddots & \\
 & & & & & 1
\end{pmatrix}
\in \mathrm{SL}_n(\mathcal{A}) \quad \text{where } Z \text{ appears } j \text{ times.}
$$

Figure 5: Diamond move.

1.3.2 Adjacent snake pairs

Definition 1.7 We say that an ordered pair (σ, σ') of snakes σ and σ' forms an *adjacent pair of snakes* if it satisfies either of the following conditions:

(1) For some $2 \leqslant k \leqslant n-1$,

    (a) $\sigma_j = \sigma'_j$ for $1 \leqslant j \leqslant k-1$ and $k+1 \leqslant j \leqslant n$,

    (b) $\sigma_k = \sigma^{\text{right}}_{k+1}(= \sigma'^{\text{right}}_{k+1})$ and $\sigma'_k = \sigma^{\text{left}}_{k+1}(= \sigma'^{\text{left}}_{k+1})$,

    in which case (σ, σ') is called an adjacent pair of *diamond-type*; see Figure 5.

(2) (a) $\sigma_j = \sigma'_j$ for $2 \leqslant j \leqslant n$,

    (b) $\sigma_1 = \sigma^{\text{right}}_2(= \sigma'^{\text{right}}_2)$ and $\sigma'_1 = \sigma^{\text{left}}_2(= \sigma'^{\text{left}}_2)$,

    in which case (σ, σ') is called an adjacent pair of *tail-type*; see Figure 6.

1.3.3 Diamond and tail moves Let (σ, σ') be an adjacent pair of snakes of diamond-type, as shown in Figure 5.

Consider the snake-vertices $\sigma_{k+1}(= \sigma'_{k+1})$, σ_k, σ'_k, and $\sigma_{k-1}(= \sigma'_{k-1})$. One checks that

$$\alpha_k = \alpha'_k = k-1, \quad \beta'_k = \beta_{k-1} = \beta_{k+1}+1, \quad \text{and} \quad \gamma_k = \gamma_{k-1} = \gamma_{k+1}+1.$$
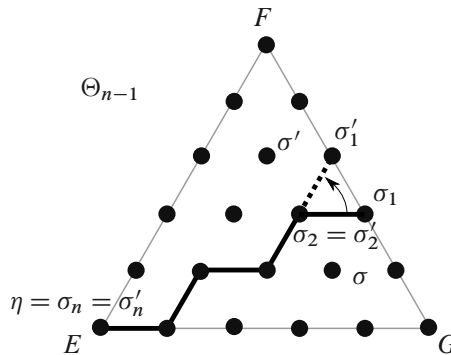
Figure 6: Tail move.

Taken together, these three coordinates form a vertex

$$(a, b, c) = (k - 1, \beta_{k+1} + 1, \gamma_{k+1} + 1) \in \mathrm{int}(\Theta_n)$$

in the interior of the n–discrete triangle Θ_n (not Θ_{n-1}), since $(k - 1) + (\beta_{k+1} + 1) + (\gamma_{k+1} + 1) = (\alpha_{k+1} + \beta_{k+1} + \gamma_{k+1}) + 1 = n$. The coordinates of this internal vertex (a, b, c) can also be thought of as delineating the boundary of a small downward-facing triangle ∇ in the discrete triangle Θ_{n-1}, whose three vertices are σ_k, σ_k', and σ_{k-1} (Figure 5). Put $X_{abc} = \tau_{abc}(E, F, G) \in \mathbb{C} - \{0\}$, namely X_{abc} is the Fock–Goncharov triangle invariant (Section 1.1.3) associated to the generic flag triple (E, F, G) and the internal vertex $(a, b, c) \in \mathrm{int}(\Theta_n)$.

The proposition below is the main ingredient going into the proof of Theorem 1.2. First, we set our conventions for change of basis matrices for bases of V^*.

Given any basis $\mathcal{U} = \{u_1, u_2, \ldots, u_n\}$ of V^*, and given a covector u in V^*, the *coordinate covector* $[u]_{\mathcal{U}}$ of the covector u with respect to the basis $\mathcal{U}$ is the unique row matrix $[u]_{\mathcal{U}} = \begin{pmatrix} y_1 & y_2 & \cdots & y_n \end{pmatrix}$ in $\mathrm{M}_{1,n}(\mathbb{C})$ such that $u = \sum_{i=1}^{n} y_i u_i$. If $\mathcal{U}' = \{u_1', u_2', \ldots, u_n'\}$ is another basis for V^*, then the *change of basis matrix* $\boldsymbol{B}_{\mathcal{U} \to \mathcal{U}'}$ going from the basis $\mathcal{U}$ to the basis $\mathcal{U}'$ is the unique invertible matrix in $\mathrm{GL}_n(\mathbb{C}) \subseteq \mathrm{M}_n(\mathbb{C})$ satisfying

$$[u]_{\mathcal{U}} \boldsymbol{B}_{\mathcal{U} \to \mathcal{U}'} = [u]_{\mathcal{U}'} \in \mathrm{M}_{1,n}(\mathbb{C}) \quad \text{for } u \in V^*.$$

Change of basis matrices satisfy the property

$$\boldsymbol{B}_{\mathcal{U} \to \mathcal{U}''} = \boldsymbol{B}_{\mathcal{U} \to \mathcal{U}'} \boldsymbol{B}_{\mathcal{U}' \to \mathcal{U}''} \in \mathrm{GL}_n(\mathbb{C}) \quad \text{for } \mathcal{U}, \mathcal{U}' \text{ and } \mathcal{U}'' \text{ bases for } V^*.$$

Proposition 1.8 (Fock and Goncharov) *Let (E, F, G) be a maximum span flag triple, (σ, σ') an adjacent pair of snakes, and $\mathcal{U}$ and $\mathcal{U}'$ the corresponding normalized projective bases of V^*, satisfying the compatibility condition $u_n = u_n' \in L_{\sigma_n} = L_\eta$.*

If (σ, σ') is of diamond-type, then the change of basis matrix $\boldsymbol{B}_{\mathcal{U} \to \mathcal{U}'} \in \mathrm{GL}_n(\mathbb{C})$ is

$$\boldsymbol{B}_{\mathcal{U} \to \mathcal{U}'} = X_{abc}^{+(k-1)/n} \boldsymbol{S}_k^{\mathrm{left}}(X_{abc}) \in \mathrm{GL}_n(\mathbb{C}) \qquad \text{(see Section 1.3.1).}$$

We say this case expresses a diamond move from the snake σ to the adjacent snake σ'.

If (σ, σ') is of tail-type, then the change of basis matrix $\boldsymbol{B}_{\mathcal{U} \to \mathcal{U}'}$ equals

$$\boldsymbol{B}_{\mathcal{U} \to \mathcal{U}'} = \boldsymbol{S}_1^{\mathrm{left}} \in \mathrm{SL}_n(\mathbb{C}) \qquad \text{(see Section 1.3.1).}$$

We say this case expresses a tail move from the snake σ to the adjacent snake σ'.

Proof See [9, Section 9]. We also provide a proof in [5, Section 2.18]. $\qquad\qquad\square$

1.3.4 Right snakes and right snake moves Our definition of a (left) snake in Section 1.2.1 took the snake-head $\eta = \sigma_n$ to be the nth snake-vertex. There is another possibility, where $\eta = \sigma_1$.

Definition 1.9 A *right n–snake* σ (for the snake-head $\eta = (n-1, 0, 0) \in \Gamma(\Theta_{n-1})$) is an ordered list $\sigma = (\sigma_1, \sigma_2, \ldots, \sigma_n) \in (\Theta_{n-1})^n$ of n–many vertices $\sigma_k = (\alpha_k, \beta_k, \gamma_k)$, satisfying

$$\alpha_k = n - k, \quad \beta_k \geqslant \beta_{k-1}, \quad \text{and} \quad \gamma_k \geqslant \gamma_{k-1} \quad \text{for } k = 1, 2, \ldots, n.$$

Right snakes for other snake-heads $\eta \in \Gamma(\Theta_{n-1})$ are similarly defined by triangular symmetry.

To adjust for using right snakes, the definitions of Sections 1.2.3, 1.3.2, and 1.3.3 need to be modified.

Given σ_{k-1}, there are two possibilities for σ_k:

$$\sigma_{k-1}^{\text{left}} = (\alpha_{k-1}^{\text{left}}, \beta_{k-1}^{\text{left}}, \gamma_{k-1}^{\text{left}}) \quad \text{for} \quad \alpha_{k-1}^{\text{left}} = n - k, \quad \beta_{k-1}^{\text{left}} = \beta_{k-1} + 1, \quad \gamma_{k-1}^{\text{left}} = \gamma_{k-1},$$

$$\sigma_{k-1}^{\text{right}} = (\alpha_{k-1}^{\text{right}}, \beta_{k-1}^{\text{right}}, \gamma_{k-1}^{\text{right}}) \quad \text{for} \quad \alpha_{k-1}^{\text{right}} = n - k, \quad \beta_{k-1}^{\text{right}} = \beta_{k-1}, \quad \gamma_{k-1}^{\text{right}} = \gamma_{k-1} + 1.$$

The algorithm defining the (ordered) projective basis $[\mathcal{U}] = [\{u_1, u_2, \ldots, u_n\}]$ becomes

(1) $u_k = -u_{k-1}^{\text{left}} \in L_{\sigma_{k-1}^{\text{left}}}$ if $\sigma_k = \sigma_{k-1}^{\text{left}}$,

(2) $u_k = +u_{k-1}^{\text{right}} \in L_{\sigma_{k-1}^{\text{right}}}$ if $\sigma_k = \sigma_{k-1}^{\text{right}}$.

In particular, the algorithm starts by making a choice of normalization covector $u_1 \in L_{\sigma_1} = L_{(n-1,0,0)}$. Notice that, compared to the setting of left snakes (Definition 1.6 and Figure 4), the signs defining the projective basis have been swapped.

An ordered pair (σ, σ') of right snakes forms an adjacent pair if either:

(1) For some $2 \leqslant k \leqslant n - 1$,

    (a) $\sigma_j = \sigma_j'$ for $1 \leqslant j \leqslant k - 1$ and $k + 1 \leqslant j \leqslant n$,

    (b) $\sigma_k = \sigma_{k-1}^{\text{left}} (= \sigma_{k-1}'^{\text{left}})$ and $\sigma_k' = \sigma_{k-1}^{\text{right}} (= \sigma_{k-1}'^{\text{right}})$,

    in which case (σ, σ') is called an adjacent pair of diamond-type.

(2) (a) $\sigma_j = \sigma_j'$ for $1 \leqslant j \leqslant n - 1$,

    (b) $\sigma_n = \sigma_{n-1}^{\text{left}} (= \sigma_{n-1}'^{\text{left}})$ and $\sigma_n' = \sigma_{n-1}^{\text{right}} (= \sigma_{n-1}'^{\text{right}})$,

    in which case (σ, σ') is called an adjacent pair of tail-type.

Given an adjacent pair (σ, σ') of right snakes of diamond-type, there is naturally associated a vertex $(a, b, c) \in \Theta_n$ to which is assigned a Fock–Goncharov triangle invariant X_{abc}.

Proposition 1.10 (Fock and Goncharov) *Let (E, F, G) be a maximum span triple, (σ, σ') an adjacent pair of right snakes, and $\mathcal{U}$ and $\mathcal{U}'$ the corresponding normalized projective bases of V^*, satisfying the compatibility condition $u_1 = u_1' \in L_{\sigma_1} = L_\eta$.*

If (σ, σ') is of diamond-type, then the change of basis matrix $\boldsymbol{B}_{\mathcal{U} \to \mathcal{U}'} \in \mathrm{GL}_n(\mathbb{C})$ equals

$$\boldsymbol{B}_{\mathcal{U} \to \mathcal{U}'} = X_{abc}^{-(k-1)/n} \boldsymbol{S}_k^{\text{right}}(X_{abc}) \in \mathrm{GL}_n(\mathbb{C}) \qquad \text{(see Section 1.3.1).}$$

If (σ, σ') is of tail-type, then the change of basis matrix $\boldsymbol{B}_{\mathcal{U} \to \mathcal{U}'}$ equals

$$\boldsymbol{B}_{\mathcal{U} \to \mathcal{U}'} = \boldsymbol{S}_1^{\text{right}} \in \mathrm{SL}_n(\mathbb{C}) \qquad \text{(see Section 1.3.1).}$$

Proof See [9, Section 9]. This is similar to the proof of Proposition 1.8. □
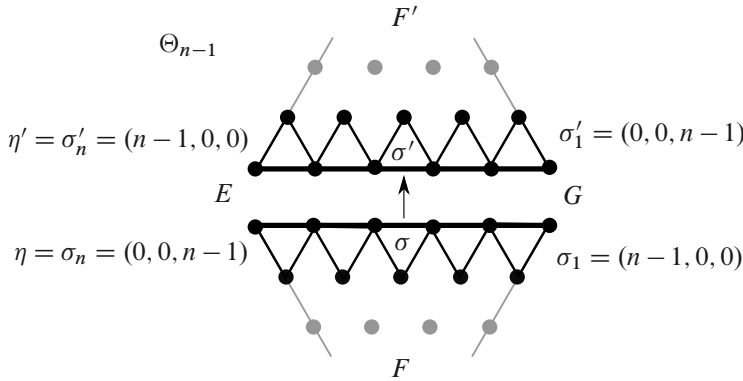
Figure 7: Edge move.

Remark 1.11 From now on, "snake" means "left snake", as in Definition 1.5, and we will say explicitly if we are using right snakes.

1.3.5 Snake moves for edges

Caution 1.12 In this subsubsection, we will consider snake-heads in the set of corner vertices $\Gamma(\Theta_{n-1})$ other than $(n-1,0,0)$, specifically η below; see Remark 1.4.

Let (E, G, F, F') be a maximum span flag quadruple; see Section 1.1.1. By Section 1.1.3, for each $j = 1, \ldots, n-1$ we may consider the Fock–Goncharov edge invariant $Z_j = \epsilon_j(E, G, F, F') \in \mathbb{C} - \{0\}$ associated to the quadruple (E, G, F, F').

Consider two copies of the discrete triangle; see Figure 7. The bottom triangle $\Theta_{n-1}(G, F, E)$ has a maximum span flag triple (G, F, E) assigned to the corner vertices $\Gamma(\Theta_{n-1})$, and the top triangle $\Theta_{n-1}(E, F', G)$ has assigned to $\Gamma(\Theta_{n-1})$ a maximum span flag triple (E, F', G).

Define (left) snakes σ and σ' in $\Theta_{n-1}(G, F, E)$ and $\Theta_{n-1}(E, F', G)$, respectively, as follows:

$$\sigma_k = (n-k, 0, k-1) \in \Theta_{n-1}(G, F, E) \quad \text{for } k = 1, \ldots, n,$$
$$\sigma'_k = (k-1, 0, n-k) \in \Theta_{n-1}(E, F', G) \quad \text{for } k = 1, \ldots, n.$$

The line decompositions associated to the snakes σ and σ' and their respective triples of flags are the same:

$$L_{\sigma_k} = L_{\sigma'_k} = (E^{(k-1)} \oplus G^{(n-k)})^{\perp} \subseteq V^* \quad \text{for } k = 1, \ldots, n.$$

Let $\mathcal{U}$ and $\mathcal{U}'$ be the associated normalized projective bases, where the normalizations are chosen in a compatible way, that is, such that $u_n = u'_n$ in $L_{\sigma_n} = L_{\sigma'_n}$.

Proposition 1.13 (Fock and Goncharov) *The change of basis matrix expressing the snake edge move* $\sigma \to \sigma'$ *is*

$$\boldsymbol{B}_{\mathcal{U}\to\mathcal{U}'} = \prod_{j=1}^{n-1} Z_j^{+j/n} \boldsymbol{S}_j^{\mathrm{edge}}(Z_j) \in \mathrm{GL}_n(\mathbb{C}) \qquad (\text{see Section 1.3.1}).$$

Proof See [9, Section 9]. This is similar to the proof of Proposition 1.8; see also [5, Section 2.22]. $\square$

1.4 Classical left, right, and edge matrices

Caution 1.14 We consider snake-heads in the set of corner vertices $\{(n-1,0,0),(0,n-1,0),(0,0,n-1)\}$ other than $(n-1,0,0)$; see Remark 1.4.

We will also consider both (left) snakes and right snakes; see Remark 1.11.

We begin the process of algebraizing the geometry discussed throughout this first section.

1.4.1 Snake sequences

Left setting Define a snake-head $\eta \in \Gamma(\Theta_{n-1})$ and two (left) snakes σ^{bot} and σ^{top}, called the bottom and top snakes, respectively, by

$$\eta = (n-1,0,0), \quad \sigma_k^{\mathrm{bot}} = (k-1,0,n-k), \quad \text{and} \quad \sigma_k^{\mathrm{top}} = (k-1,n-k,0) \quad \text{for } k = 1,\ldots,n.$$

Right setting Define η and right snakes σ^{bot} and σ^{top} by

$$\eta = (0,0,n-1), \quad \sigma_k^{\mathrm{bot}} = (k-1,0,n-k), \quad \text{and} \quad \sigma_k^{\mathrm{top}} = (0,k-1,n-k) \quad \text{for } k = 1,\ldots,n.$$

In either left or right setting, consider a sequence $\sigma^{\mathrm{bot}} = \sigma^1, \sigma^2, \ldots, \sigma^{N-1}, \sigma^N = \sigma^{\mathrm{top}}$ of snakes having the same snake-head η as σ^{bot} and σ^{top}, such that (σ^l, σ^{l+1}) is an adjacent pair; see Figure 8. Note that this sequence of snakes is not in general unique. For the N–many projective bases $[\mathcal{U}^l] = [\{u_1^l, u_2^l, \ldots, u_n^l\}]$ associated to the snakes σ^l, choose a common normalization $u_n^l := u_n \in L_\eta$ (resp. $u_1^l := u_1 \in L_\eta$), where the same u_n (resp. u_1) is used for all l, when working in the left (resp. right) setting. Then, the change of basis matrix $\boldsymbol{B}_{\mathcal{U}^{\mathrm{bot}} \to \mathcal{U}^{\mathrm{top}}}$ can be decomposed as (see Section 1.3.3)

$$(*) \qquad \boldsymbol{B}_{\mathcal{U}^{\mathrm{bot}} \to \mathcal{U}^{\mathrm{top}}} = \boldsymbol{B}_{\mathcal{U}^1 \to \mathcal{U}^2} \boldsymbol{B}_{\mathcal{U}^2 \to \mathcal{U}^3} \cdots \boldsymbol{B}_{\mathcal{U}^{N-1} \to \mathcal{U}^N} \in \mathrm{GL}_n(\mathbb{C}).$$
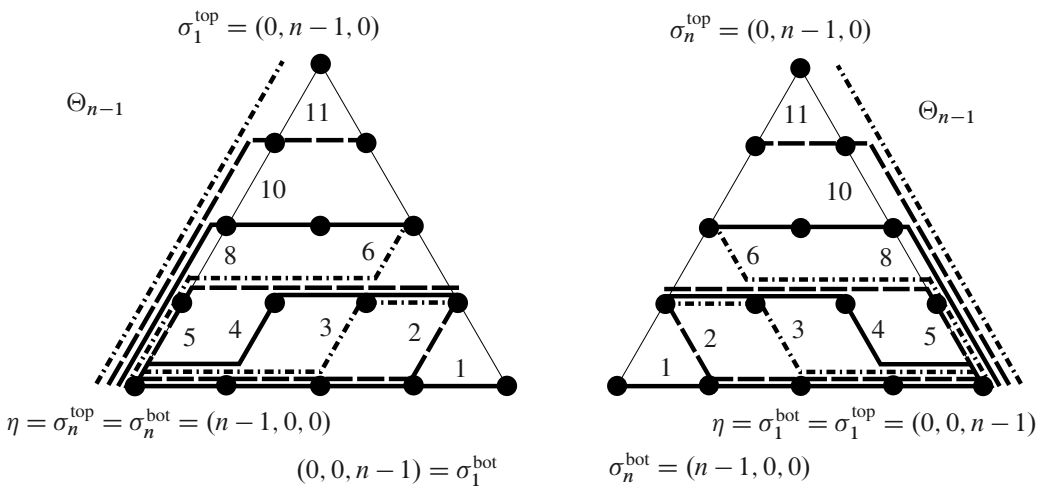
Figure 8: Classical snake sweep for $n = 5$. The preferred choices for the left and right snake sequences are on the left and right, respectively.
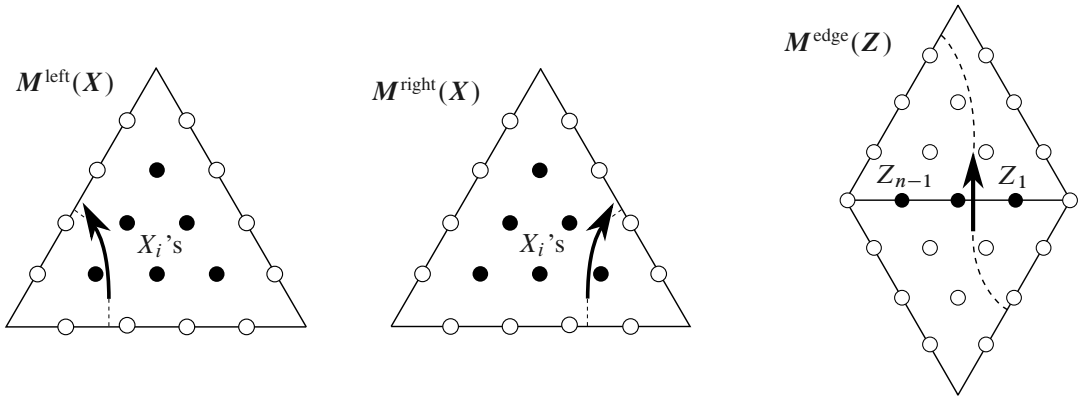
Figure 9: Classical matrices (viewed from the Θ_n–perspective): from left to right, the left, right, and edge matrices.

Here the matrices $\boldsymbol{B}_{\mathcal{U}^l \to \mathcal{U}^{l+1}}$ are computed as in [Proposition 1.8](#) (resp. [Proposition 1.10](#)) in the left (resp. right) setting, and in particular are completely determined by the Fock–Goncharov triangle invariants $X_{abc} \in \mathbb{C} - \{0\}$ associated to the internal vertices $(a, b, c) \in \mathrm{int}(\Theta_n)$ of the n–discrete triangle.

Note that the matrix $\boldsymbol{B}_{\mathcal{U}^{\mathrm{bot}} \to \mathcal{U}^{\mathrm{top}}}$ is, by definition, independent of the choice of snake sequence $(\sigma^l)_l$. For concreteness, throughout we make a preferred choice of such sequence, depending on whether we are in the left or right setting; see [Figure 8](#).

1.4.2 Algebraization

Let $\mathcal{A}$ be a commutative algebra ([Section 1.3.1](#)). For $i = 1, 2, \ldots, \frac{1}{2}(n-1)(n-2)$, let $X_i^{1/n} \in \mathcal{A}$ and put $X_i = (X_i^{1/n})^n$. For $j = 1, 2, \ldots, n-1$, let $Z_j^{1/n} \in \mathcal{A}$ and put $Z_j = (Z_j^{1/n})^n$. Note, $\frac{1}{2}(n-1)(n-2)$ is the number of elements $(a, b, c) \in \mathrm{int}(\Theta_n)$, which we arbitrarily enumerate $1, 2, \ldots, \frac{1}{2}(n-1)(n-2)$; see [Figure 9](#), left and center. And note that $n-1$ is the number of noncorner vertices of Θ_n lying on a single edge, which we enumerate $1, 2, \ldots, n-1$ as shown in [Figure 9](#), right. Let $\boldsymbol{X} = (X_i)_i$ and $\boldsymbol{Z} = (Z_j)_j$ be the corresponding tuples of these elements of $\mathcal{A}$.

As a notational convention, given a family $M_l \in \mathrm{M}_n(\mathcal{A})$ of $n \times n$ matrices, put

$$
\prod_{l=m}^{p} M_l = M_m M_{m+1} \cdots M_p, \qquad \prod_{l=p+1}^{m} M_l = 1 \quad \text{for } m \leqslant p,
$$

$$
\coprod_{l=p}^{m} M_l = M_p M_{p-1} \cdots M_m, \qquad \coprod_{l=m-1}^{p} M_l = 1 \quad \text{for } m \leqslant p.
$$

Definition 1.15 The *left matrix* $\boldsymbol{M}^{\mathrm{left}}(\boldsymbol{X})$ in $\mathrm{SL}_n(\mathcal{A})$ is defined by

$$
\boldsymbol{M}^{\mathrm{left}}(\boldsymbol{X}) = \coprod_{k=n-1}^{1} \left(S_1^{\mathrm{left}} \prod_{l=2}^{k} S_l^{\mathrm{left}}(X_{(l-1)(n-k)(k-l+1)}) \right) \in \mathrm{SL}_n(\mathcal{A}),
$$

where the matrix $S_l^{\mathrm{left}}(X_{abc})$ is the lth left-elementary matrix; see [Section 1.3.1](#).

Similarly, the *right matrix* $\boldsymbol{M}^{\text{right}}(X)$ in $\text{SL}_n(\mathcal{A})$ is defined by

$$\boldsymbol{M}^{\text{right}}(X) = \coprod_{k=n-1}^{1} \left(\boldsymbol{S}_1^{\text{right}} \prod_{l=2}^{k} \boldsymbol{S}_l^{\text{right}}(X_{(k-l+1)(n-k)(l-1)}) \right) \in \text{SL}_n(\mathcal{A}),$$

where the matrix $\boldsymbol{S}_l^{\text{right}}(X_{abc})$ is the lth right-elementary matrix; see Section 1.3.1.

Lastly, the *edge matrix* $\boldsymbol{M}^{\text{edge}}(Z)$ in $\text{SL}_n(\mathcal{A})$ is defined by

$$\boldsymbol{M}^{\text{edge}}(Z) = \prod_{l=1}^{n-1} \boldsymbol{S}_l^{\text{edge}}(Z_l) \in \text{SL}_n(\mathcal{A}),$$

where the matrix $\boldsymbol{S}_l^{\text{edge}}(Z_l)$ is the lth edge-elementary matrix; see Section 1.3.1. See Figure 9.

Remark 1.16 In the case where $\mathcal{A} = \mathbb{C}$ and the $X_i = \tau_{abc}(E, F, G)$ and $Z_j = \epsilon_j(E, G, F, F')$ in $\mathbb{C} - \{0\}$ are the triangle and edge invariants (as in Sections 1.3.3, 1.3.4, and 1.3.5), then the left and right matrices $\boldsymbol{M}^{\text{left}}(X)$ and $\boldsymbol{M}^{\text{right}}(X)$ are the normalized change of basis matrix $\boldsymbol{B}_{\mathcal{U}^{\text{bot}} \to \mathcal{U}^{\text{top}}} / \text{Det}^{1/n}$ (see (∗)) in the left and right settings, respectively, normalized to have determinant 1, and decomposed in terms of our preferred snake sequence (Figure 8). Also, the edge matrix $\boldsymbol{M}^{\text{edge}}(Z)$ is the normalization $\boldsymbol{B}_{\mathcal{U} \to \mathcal{U}'} / \text{Det}^{1/n}$ of the change of basis matrix from Proposition 1.13. Note, these normalizations require choosing n–roots of the invariants X_i and Z_j.

2 Quantum matrices

Although we will not use explicitly the geometric results of the previous section, those results motivate the algebraic objects that are our main focus.

Throughout, let $q \in \mathbb{C} - \{0\}$ and $\omega = q^{1/n^2}$ be a n^2–root of q. Technically, also choose $\omega^{1/2}$.

2.1 Quantum tori, matrix algebras, and the Weyl quantum ordering

2.1.1 Quantum tori Let $\boldsymbol{P}$ (for "Poisson") be an integer $N \times N$ antisymmetric matrix.

Definition 2.1 The *quantum torus* (*with n–roots*) $\mathcal{T}^\omega(\boldsymbol{P})$ associated to $\boldsymbol{P}$ is the quotient of the free algebra $\mathbb{C}\{X_1^{1/n}, X_1^{-1/n}, \dots, X_N^{1/n}, X_N^{-1/n}\}$ in the indeterminates $X_i^{\pm 1/n}$ by the two-sided ideal generated by the relations

$$X_i^{1/n} X_j^{1/n} = \omega^{\boldsymbol{P}_{ij}} X_j^{1/n} X_i^{1/n} \quad \text{and} \quad X_i^{1/n} X_i^{-1/n} = X_i^{-1/n} X_i^{1/n} = 1.$$

Put $X_i^{\pm 1} = (X_i^{\pm 1/n})^n$. We refer to the $X_i^{\pm 1/n}$ as *generators*, and the X_i as *quantum coordinates*, or just *coordinates*. Define the subset of fractions

$$\mathbb{Z}/n = \left\{ \frac{m}{n} \,\middle|\, m \in \mathbb{Z} \right\} \subseteq \mathbb{Q}.$$

Written in terms of the coordinates X_i and the fractions $r \in \mathbb{Z}/n$, we have the relations

$$X_i^{r_i} X_j^{r_j} = q^{\boldsymbol{P}_{ij} r_i r_j} X_j^{r_j} X_i^{r_i} \quad \text{for } r_i, r_j \in \mathbb{Z}/n.$$

2.1.2 Matrix algebras

Definition 2.2 The *matrix algebra* M$_n$($\mathcal{T}$) with coefficients in a possibly noncommutative algebra $\mathcal{T}$ is the vector space of $n \times n$ matrices, equipped with the usual multiplicative structure. Namely, the product MN of two matrices M and N is defined entrywise by

$$(MN)_{ij} = \sum_{k=1}^{n} M_{ik} N_{kj} \in \mathcal{T} \quad \text{for } 1 \leqslant i, j \leqslant n.$$

Here we use the usual convention that the entry M_{ij} of a matrix M is the entry in the ith row and j^{th} column. Note that the order of M_{ik} and N_{kj} in the above equation matters since these elements might not commute in $\mathcal{T}$.

2.1.3 Weyl quantum ordering
If $\mathcal{T}$ is a quantum torus, then there is a linear map

$$[-] : \mathbb{C}\{X_1^{1/n}, X_1^{-1/n}, \ldots, X_N^{1/n}, X_N^{-1/n}\} \to \mathcal{T}$$

from the free algebra to $\mathcal{T}$, called the *Weyl quantum ordering*, defined by the property that a word $X_{i_1}^{r_1} X_{i_2}^{r_2} \cdots X_{i_k}^{r_k}$ for $r_a \in \mathbb{Z}/n$ (note that i_a may equal i_b if $a \neq b$) is mapped to

$$[X_{i_1}^{r_1} X_{i_2}^{r_2} \cdots X_{i_k}^{r_k}] = (q^{-\frac{1}{2} \sum_{1 \leqslant a < b \leqslant k} P_{i_a i_b} r_a r_b}) X_{i_1}^{r_1} X_{i_2}^{r_2} \cdots X_{i_k}^{r_k},$$

where on the right-hand side we implicitly mean the equivalence class in $\mathcal{T}$. Also, the empty word is mapped to 1. Note that the Weyl ordering $[-]$ depends on the choice of $\omega^{1/2}$; see the beginning of Section 2.

The Weyl ordering is specially designed to satisfy the symmetry

$$[X_{i_1}^{r_1} X_{i_2}^{r_2} \cdots X_{i_k}^{r_k}] = [X_{i_{\sigma(1)}}^{r_{\sigma(1)}} X_{i_{\sigma(2)}}^{r_{\sigma(2)}} \cdots X_{i_{\sigma(k)}}^{r_{\sigma(k)}}]$$

for every permutation σ of $\{1, \ldots, k\}$; see [1]. Also, $[X_i^{1/n} X_i^{-1/n}] = 1$. Consequently, a linear map

$$[-] : \mathbb{C}[X_1^{\pm 1/n}, \ldots, X_N^{\pm 1/n}] \to \mathcal{T}$$

is induced from the commutative Laurent polynomial algebra to $\mathcal{T}$. This determines a linear map of matrix algebras

$$[-] : \mathrm{M}_n(\mathbb{C}[X_1^{\pm 1/n}, \ldots, X_N^{\pm 1/n}]) \to \mathrm{M}_n(\mathcal{T}) \quad \text{given by } [M]_{ij} = [M_{ij}] \text{ in } \mathcal{T}.$$

2.2 Fock–Goncharov quantum torus for a triangle

Let $\Gamma(\Theta_n)$ denote the set of corner vertices $\Gamma(\Theta_n) = \{(n, 0, 0), (0, n, 0), (0, 0, n)\}$ of the discrete triangle Θ_n; see Section 1.1.2.

Define a function

$$P : (\Theta_n - \Gamma(\Theta_n)) \times (\Theta_n - \Gamma(\Theta_n)) \to \{-2, -1, 0, 1, 2\}$$

using the *quiver* with vertex set $\Theta_n - \Gamma(\Theta_n)$ illustrated in Figure 10. The function P is defined by sending the ordered tuple (v_1, v_2) of vertices of $\Theta_n - \Gamma(\Theta_n)$ to 2 (resp. -2) if there is a solid arrow pointing from v_1 to v_2 (resp. v_2 to v_1), to 1 (resp. -1) if there is a dotted arrow pointing from v_1 to v_2 (resp. v_2 to v_1),
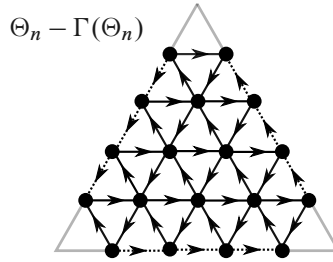
Figure 10: Quiver defining the Fock–Goncharov quantum torus.

and to 0 if there is no arrow connecting ν_1 and ν_2. Note that all of the small downward-facing triangles are oriented clockwise, and all of the small upward-facing triangles are oriented counterclockwise. By labeling the vertices of $\Theta_n - \Gamma(\Theta_n)$ by their coordinates (a, b, c) we may think of the function $\boldsymbol{P}$ as an $N \times N$ antisymmetric matrix $\boldsymbol{P} = (\boldsymbol{P}_{abc,a'b'c'})$, called the *Poisson matrix* associated to the quiver. Here $N = 3(n-1) + \frac{1}{2}(n-1)(n-2)$; compare with Section 1.4.2.

Definition 2.3 Define the *Fock–Goncharov quantum torus*

$$\mathcal{T}_n^\omega = \mathbb{C}[X_1^{\pm 1/n}, X_2^{\pm 1/n}, \ldots, X_N^{\pm 1/n}]^\omega$$

associated to the discrete *n*–triangle Θ_n to be the quantum torus $\mathcal{T}^\omega(\boldsymbol{P})$ defined by the $N \times N$ Poisson matrix $\boldsymbol{P}$, with generators $X_i^{\pm 1/n} = X_{abc}^{\pm 1/n}$ for all $(a, b, c) \in \Theta_n - \Gamma(\Theta_n)$. Note that when $q = \omega = 1$ this recovers the classical Laurent polynomial algebra $\mathcal{T}_n^1 = \mathbb{C}[X_1^{\pm 1/n}, X_2^{\pm 1/n}, \ldots, X_N^{\pm 1/n}]$.

As a notational convention, for $j = 1, 2, \ldots, n-1$ we write $Z_j^{\pm 1/n}$ (resp. $Z_j'^{\pm 1/n}$ and $Z_j''^{\pm 1/n}$) in place of $X_{j0(n-j)}^{\pm 1/n}$ (resp. $X_{j(n-j)0}^{\pm 1/n}$ and $X_{0j(n-j)}^{\pm 1/n}$); see Figure 11. So, *triangle-coordinates* will be denoted by $X_i = X_{abc}$ for $(a, b, c) \in \text{int}(\Theta_n)$ while *edge-coordinates* will be denoted by Z_j, Z_j', and Z_j''.

2.3   Quantum left and right matrices

2.3.1   Weyl quantum ordering for the Fock–Goncharov quantum torus   Let $\mathcal{T} = \mathcal{T}_n^\omega$ be the Fock–Goncharov quantum torus (Section 2.2). Then the Weyl ordering $[-]$ of Section 2.1.3 gives a map

$$[-]: \mathrm{M}_n(\mathcal{T}_n^1) \to \mathrm{M}_n(\mathcal{T}_n^\omega),$$

where we have used the identification $\mathcal{T}_n^1 = \mathbb{C}[X_1^{\pm 1/n}, X_2^{\pm 1/n}, \ldots, X_N^{\pm 1/n}]$ discussed in Section 2.2.

2.3.2   Quantum left and right matrices   For a commutative algebra $\mathcal{A}$, in Section 1.4.2 we defined the classical matrices $\boldsymbol{M}^{\text{left}}(\boldsymbol{X})$, $\boldsymbol{M}^{\text{right}}(\boldsymbol{X})$, and $\boldsymbol{M}^{\text{edge}}(\boldsymbol{Z})$ in $\mathrm{SL}_n(\mathcal{A})$. If $\mathcal{A} = \mathbb{C}[X_1^{\pm 1/n}, \ldots, X_N^{\pm 1/n}] = \mathcal{T}_n^1$, we now use these matrices to define the primary objects of study.

Definition 2.4   Put vectors $\boldsymbol{X} = (X_i)$, $\boldsymbol{Z} = (Z_j)$, $\boldsymbol{Z}' = (Z_j')$, $\boldsymbol{Z}'' = (Z_j'')$ as in Figure 11. We define the *quantum left matrix* $\boldsymbol{L}^\omega$ in $\mathrm{M}_n(\mathcal{T}_n^\omega)$ by the formula

$$\boldsymbol{L}^\omega = \boldsymbol{L}^\omega(\boldsymbol{Z}, \boldsymbol{X}, \boldsymbol{Z}') = [\boldsymbol{M}^{\text{edge}}(\boldsymbol{Z})\boldsymbol{M}^{\text{left}}(\boldsymbol{X})\boldsymbol{M}^{\text{edge}}(\boldsymbol{Z}')] \in \mathrm{M}_n(\mathcal{T}_n^\omega),$$
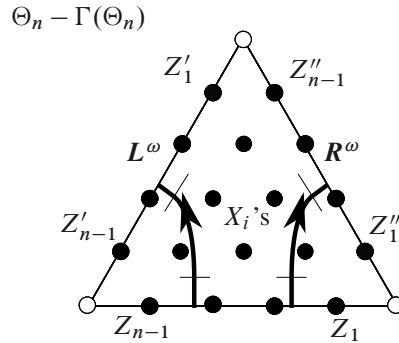
Figure 11: Quantum left and right matrices (compare with Figure 9).

where we have applied the Weyl quantum ordering $[-]$ discussed in Section 2.3.1 to the product $\boldsymbol{M}^{\mathrm{edge}}(\boldsymbol{Z})\boldsymbol{M}^{\mathrm{left}}(\boldsymbol{X})\boldsymbol{M}^{\mathrm{edge}}(\boldsymbol{Z}')$ of classical matrices in $\mathrm{M}_n(\mathcal{T}_n^1)$. In other words, we apply the Weyl ordering to each entry of the classical matrix.

Similarly, as in Figure 11, we define the *quantum right matrix* $\boldsymbol{R}^{\omega}$ in $\mathrm{M}_n(\mathcal{T}_n^{\omega})$ by

$$\boldsymbol{R}^{\omega} = \boldsymbol{R}^{\omega}(\boldsymbol{Z}, \boldsymbol{X}, \boldsymbol{Z}'') = [\boldsymbol{M}^{\mathrm{edge}}(\boldsymbol{Z})\boldsymbol{M}^{\mathrm{right}}(\boldsymbol{X})\boldsymbol{M}^{\mathrm{edge}}(\boldsymbol{Z}'')] \in \mathrm{M}_n(\mathcal{T}_n^{\omega}).$$

2.4 Main result

2.4.1 Quantum SL_n and its points
Let $\mathcal{T}$ be a possibly noncommutative algebra.

Definition 2.5 We say that a 2×2 matrix $\boldsymbol{M} = \begin{pmatrix} a & b \\ c & d \end{pmatrix}$ in $\mathrm{M}_2(\mathcal{T})$ is a $\mathcal{T}$–*point of the quantum matrix algebra* M_2^q, denoted by $\boldsymbol{M} \in \mathrm{M}_2^q(\mathcal{T}) \subseteq \mathrm{M}_2(\mathcal{T})$, if

$(**)$ $ba = qab, \quad dc = qcd, \quad ca = qac, \quad db = qbd, \quad bc = cb, \quad da - ad = (q - q^{-1})bc$ in $\mathcal{T}$.

We say that a matrix $\boldsymbol{M} \in \mathrm{M}_2(\mathcal{T})$ is a $\mathcal{T}$–*point of the quantum special linear group* SL_2^q, denoted by $\boldsymbol{M} \in \mathrm{SL}_2^q(\mathcal{T}) \subseteq \mathrm{M}_2^q(\mathcal{T}) \subseteq \mathrm{M}_2(\mathcal{T})$, if $\boldsymbol{M} \in \mathrm{M}_2^q(\mathcal{T})$ and the *quantum determinant*

$$\mathrm{Det}^q(\boldsymbol{M}) = ad - q^{-1}bc = 1 \in \mathcal{T}.$$

These notions are also defined for $n \times n$ matrices, as follows:

Definition 2.6 A matrix $\boldsymbol{M} \in \mathrm{M}_n(\mathcal{T})$ is a $\mathcal{T}$–*point of the quantum matrix algebra* M_n^q, denoted by $\boldsymbol{M} \in \mathrm{M}_n^q(\mathcal{T}) \subseteq \mathrm{M}_n(\mathcal{T})$, if every 2×2 submatrix of $\boldsymbol{M}$ is a $\mathcal{T}$–point of M_2^q. That is,

$$\boldsymbol{M}_{im}\boldsymbol{M}_{ik} = q\boldsymbol{M}_{ik}\boldsymbol{M}_{im}, \quad \boldsymbol{M}_{jm}\boldsymbol{M}_{im} = q\boldsymbol{M}_{im}\boldsymbol{M}_{jm}, \quad \boldsymbol{M}_{im}\boldsymbol{M}_{jk} = \boldsymbol{M}_{jk}\boldsymbol{M}_{im},$$

$$\boldsymbol{M}_{jm}\boldsymbol{M}_{ik} - \boldsymbol{M}_{ik}\boldsymbol{M}_{jm} = (q - q^{-1})\boldsymbol{M}_{im}\boldsymbol{M}_{jk},$$

for all $i < j$ and $k < m$, where $1 \leqslant i, j, k, m \leqslant n$.

The *quantum determinant* $\mathrm{Det}^q(\boldsymbol{M}) \in \mathcal{T}$ of a matrix $\boldsymbol{M} \in \mathrm{M}_n(\mathcal{T})$ is

$$\mathrm{Det}^q(\boldsymbol{M}) = \sum_{\sigma \in \mathfrak{S}_n} (-q^{-1})^{l(\sigma)} \boldsymbol{M}_{1\sigma(1)} \boldsymbol{M}_{2\sigma(2)} \cdots \boldsymbol{M}_{n\sigma(n)},$$

where the length $l(\sigma)$ of the permutation σ is the minimum number of factors appearing in a decomposition of σ as a product of adjacent transpositions $(i, i + 1)$; see, for example, [2, Chapter I.2].

A matrix $\boldsymbol{M} \in \mathrm{M}_n(\mathcal{T})$ is a $\mathcal{T}$–*point of the quantum special linear group* SL_n^q, denoted by $\boldsymbol{M} \in \mathrm{SL}_n^q(\mathcal{T}) \subseteq \mathrm{M}_n^q(\mathcal{T}) \subseteq \mathrm{M}_n(\mathcal{T})$, if both $\boldsymbol{M} \in \mathrm{M}_n^q(\mathcal{T})$ and $\mathrm{Det}^q(\boldsymbol{M}) = 1$.

Remark 2.7 (1) It follows from the definitions that if a $\mathcal{T}$–point $\boldsymbol{M} \in \mathrm{M}_n^q(\mathcal{T}) \subseteq \mathrm{M}_n(\mathcal{T})$ is a triangular matrix, then the diagonal entries $\boldsymbol{M}_{ii} \in \mathcal{T}$ commute and $\mathrm{Det}^q(\boldsymbol{M}) = \prod_i \boldsymbol{M}_{ii} \in \mathcal{T}$.

(2) The subsets $\mathrm{M}_n^q(\mathcal{T}) \subseteq \mathrm{M}_n(\mathcal{T})$ and $\mathrm{SL}_n^q(\mathcal{T}) \subseteq \mathrm{M}_n^q(\mathcal{T})$ are generally not closed under matrix multiplication (see, however, the proof sketch below for a relaxed property).

(3) More abstractly, the *quantum special linear group* SL_n^q is the noncommutative algebra defined as the quotient of the free algebra on generators $\boldsymbol{m}_{ij}$ for $1 \leqslant i, j \leqslant n$ subject to the four relations appearing in Definition 2.6 (with $\boldsymbol{M}_{ij}$ replaced by $\boldsymbol{m}_{ij}$) plus the relation $\mathrm{Det}^q(\boldsymbol{m}) = 1$; see, for example, [2, Chapter I.2]. Note then that a $\mathcal{T}$–point $\boldsymbol{M}$ of SL_n^q is equivalent to an algebra homomorphism $\varphi(\boldsymbol{M}) \colon \mathrm{SL}_n^q \to \mathcal{T}$ defined by the property that $\varphi(\boldsymbol{M})(\boldsymbol{m}_{ij}) = \boldsymbol{M}_{ij}$ for all $1 \leqslant i, j \leqslant n$.

2.4.2 **Main result** Take $\mathcal{T} = \mathcal{T}_n^\omega$ to be the Fock–Goncharov quantum torus for the discrete n–triangle Θ_n; see Section 2.2. Let $\boldsymbol{L}^\omega$ and $\boldsymbol{R}^\omega$ in $\mathrm{M}_n(\mathcal{T}_n^\omega)$ be the quantum left and right matrices, respectively, as defined in Definition 2.4.

Theorem 2.8 *The quantum left and right matrices*

$$\boldsymbol{L}^\omega = \boldsymbol{L}^\omega(\boldsymbol{Z}, \boldsymbol{X}, \boldsymbol{Z}') \quad \text{and} \quad \boldsymbol{R}^\omega = \boldsymbol{R}^\omega(\boldsymbol{Z}, \boldsymbol{X}, \boldsymbol{Z}'') \in \mathrm{M}_n(\mathcal{T}_n^\omega)$$

are $\mathcal{T}_n^\omega$–points of the quantum special linear group SL_n^q. That is, $\boldsymbol{L}^\omega, \boldsymbol{R}^\omega \in \mathrm{SL}_n^q(\mathcal{T}_n^\omega) \subseteq \mathrm{M}_n(\mathcal{T}_n^\omega)$.

The proof, provided in Section 3, uses a quantum version of Fock–Goncharov snakes (Section 1).

Sketch of proof (see Section 3 for more details) In the case $n = 2$, this is an enjoyable calculation. When $n \geqslant 3$, the argument hinges on the following well-known fact (see for example [21, Proposition IV.3.4 and Section IV.10]): if $\mathcal{T}$ is an algebra with subalgebras $\mathcal{T}', \mathcal{T}'' \subseteq \mathcal{T}$ that commute in the sense that $a'a'' = a''a'$ for all $a' \in \mathcal{T}'$ and $a'' \in \mathcal{T}''$, and if $\boldsymbol{M}' \in \mathrm{M}_n(\mathcal{T}') \subseteq \mathrm{M}_n(\mathcal{T})$ and $\boldsymbol{M}'' \in \mathrm{M}_n(\mathcal{T}'') \subseteq \mathrm{M}_n(\mathcal{T})$ are $\mathcal{T}$–points of SL_n^q, then the matrix product (Definition 2.2) $\boldsymbol{M}'\boldsymbol{M}'' \in \mathrm{M}_n(\mathcal{T}'\mathcal{T}'') \subseteq \mathrm{M}_n(\mathcal{T})$ is also a $\mathcal{T}$–point of SL_n^q.

Put $\boldsymbol{M}_{\mathrm{FG}} := \boldsymbol{L}^\omega$, the quantum left matrix, say. The proof is the same for the quantum right matrix. See Definition 2.4. The strategy is to see $\boldsymbol{M}_{\mathrm{FG}} \in \mathrm{M}_n(\mathcal{T}_n^\omega)$ as the product of simpler matrices, over mutually commuting subalgebras, that are themselves points of SL_n^q.

More precisely, for a fixed sequence of adjacent snakes $\sigma^{\mathrm{bot}} = \sigma^1, \sigma^2, \dots, \sigma^N = \sigma^{\mathrm{top}}$ moving left across the triangle from the bottom edge to the top-left edge, we will define for each $i = 1, \dots, N - 1$ an auxiliary algebra $\mathcal{S}_{j_i}^\omega$, called a *snake-move algebra*, for $j_i \in \{1, \dots, n - 1\}$, corresponding to the adjacent snake pair (σ^i, σ^{i+1}). As a technical step, there is a distinguished subalgebra $\mathcal{T}_L \subseteq \mathcal{T}_n^\omega$ satisfying $\boldsymbol{M}_{\mathrm{FG}} \in \mathrm{M}_n(\mathcal{T}_L) \subseteq \mathrm{M}_n(\mathcal{T}_n^\omega)$. We construct an algebra embedding $\mathcal{T}_L \hookrightarrow \bigotimes_i \mathcal{S}_{j_i}^\omega$. Through this embedding, we may view $\boldsymbol{M}_{\mathrm{FG}} \in \mathrm{M}_n(\mathcal{T}_L) \subseteq \mathrm{M}_n\big(\bigotimes_i \mathcal{S}_{j_i}^\omega\big)$.
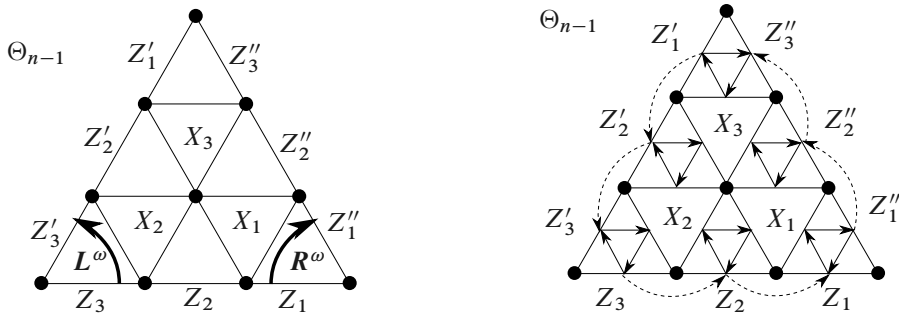
Figure 12: Quantum matrices and quantum torus for $n = 4$. Left and right matrices (left) and the quiver (right).

We construct (Proposition 3.3), for each i, a matrix $\boldsymbol{M}_{j_i} \in \mathrm{M}_n(\mathcal{S}_{j_i}^\omega) \subseteq \mathrm{M}_n(\bigotimes_i \mathcal{S}_{j_i}^\omega)$ such that $\boldsymbol{M}_{j_i}$ is an $\mathcal{S}_{j_i}^\omega$–point of SL$_n^q$; in other words $\boldsymbol{M}_{j_i} \in \mathrm{SL}_n^q(\mathcal{S}_{j_i}^\omega) \subseteq \mathrm{SL}_n^q(\bigotimes_i \mathcal{S}_{j_i}^\omega)$. Since by definition the subalgebras $\mathcal{S}_{j_i}^\omega, \mathcal{S}_{j_{i'}}^\omega \subseteq \bigotimes_i \mathcal{S}_{j_i}^\omega$ commute if $i \neq i'$ as they constitute different tensor factors of $\bigotimes_i \mathcal{S}_{j_i}^\omega$, it follows from the essential fact mentioned above that $\boldsymbol{M} := \boldsymbol{M}_{j_1} \boldsymbol{M}_{j_2} \cdots \boldsymbol{M}_{j_{N-1}} \in \mathrm{M}_n(\bigotimes_i \mathcal{S}_{j_i}^\omega)$ is a $(\bigotimes_i \mathcal{S}_{j_i}^\omega)$–point of SL$_n^q$; in other words $\boldsymbol{M} \in \mathrm{SL}_n^q(\bigotimes_i \mathcal{S}_{j_i}^\omega)$.

Since this matrix product $\boldsymbol{M}$, as well as the quantum left matrix $\boldsymbol{M}_{\mathrm{FG}}$, is being viewed as an element of $\mathrm{M}_n(\bigotimes_i \mathcal{S}_{j_i}^\omega)$, it makes sense to ask whether $\boldsymbol{M}_{\mathrm{FG}} \overset{?}{=} \boldsymbol{M} \in \mathrm{M}_n(\bigotimes_i \mathcal{S}_{j_i}^\omega)$. We show that this is true, implying that $\boldsymbol{M}_{\mathrm{FG}} \in \mathrm{SL}_n^q(\bigotimes_i \mathcal{S}_{j_i}^\omega)$. Since $\boldsymbol{M}_{\mathrm{FG}} \in \mathrm{M}_n(\mathcal{T}_L) \subseteq \mathrm{M}_n(\bigotimes_i \mathcal{S}_{j_i}^\omega)$, we conclude that $\boldsymbol{M}_{\mathrm{FG}}$ is in $\mathrm{SL}_n^q(\mathcal{T}_L) \subseteq \mathrm{SL}_n^q(\mathcal{T}_n^\omega)$. $\qquad\square$

2.5 Example

Consider the case $n = 4$; see Figure 12. On the right-hand side is the quiver defining the commutation relations in the quantum torus $\mathcal{T}_4^\omega$, recalling Figure 10, but viewed in Θ_{n-1}. Note that there is a one-to-one correspondence between points $(a, b, c) \in \mathrm{int}(\Theta_n)$ and small downward-facing triangles inside Θ_{n-1}; see Figure 12. In particular, to each downward-facing triangle there is associated a triangle-coordinate X_i.

Some sample commutation relations in $\mathcal{T}_4^\omega$ are

$$X_3 Z_2'' = q^2 X_3 Z_2'', \quad X_3 X_1 = q^{-2} X_1 X_3, \quad Z_3 Z_2 = q Z_2 Z_3, \quad \text{and} \quad Z_3 Z_3' = q^2 Z_3' Z_3.$$

Then, the quantum left and right matrices $\boldsymbol{L}^\omega$ and $\boldsymbol{R}^\omega$ are computed as

$$\boldsymbol{L}^\omega = \left[Z_1^{-\frac{1}{4}} Z_2^{-\frac{2}{4}} Z_3^{-\frac{3}{4}} \begin{pmatrix} Z_1 Z_2 Z_3 & & & \\ & Z_2 Z_3 & & \\ & & Z_3 & \\ & & & 1 \end{pmatrix} \begin{pmatrix} 1 & 1 & & \\ & 1 & & \\ & & 1 & \\ & & & 1 \end{pmatrix} X_1^{-\frac{1}{4}} \begin{pmatrix} X_1 & & & \\ & 1 & 1 & \\ & & 1 & \\ & & & 1 \end{pmatrix} X_2^{-\frac{2}{4}} \begin{pmatrix} X_2 & & & \\ & X_2 & & \\ & & 1 & 1 \\ & & & 1 \end{pmatrix} \right.$$

$$\left. \begin{pmatrix} 1 & 1 & & \\ & 1 & & \\ & & 1 & \\ & & & 1 \end{pmatrix} X_3^{-\frac{1}{4}} \begin{pmatrix} X_3 & & & \\ & 1 & 1 & \\ & & 1 & \\ & & & 1 \end{pmatrix} \begin{pmatrix} 1 & 1 & & \\ & 1 & & \\ & & 1 & \\ & & & 1 \end{pmatrix} Z_1'^{-\frac{1}{4}} Z_2'^{-\frac{2}{4}} Z_3'^{-\frac{3}{4}} \begin{pmatrix} Z_1' Z_2' Z_3' & & & \\ & Z_2' Z_3' & & \\ & & Z_3' & \\ & & & 1 \end{pmatrix} \right]$$

and

$$
\boldsymbol{R}^{\omega} = \left[Z_1^{-\frac{1}{4}} Z_2^{-\frac{2}{4}} Z_3^{-\frac{3}{4}} \begin{pmatrix} Z_1 Z_2 Z_3 & & & \\ & Z_2 Z_3 & & \\ & & Z_3 & \\ & & & 1 \end{pmatrix} \begin{pmatrix} 1 & & & \\ & 1 & & \\ & & 1 & \\ & & 1 & 1 \end{pmatrix} X_2^{+\frac{1}{4}} \begin{pmatrix} 1 & & & \\ & 1 & & \\ & 1 & 1 & \\ & & & X_2^{-1} \end{pmatrix} X_1^{+\frac{2}{4}} \begin{pmatrix} 1 & & & \\ 1 & 1 & & \\ & & X_1^{-1} & \\ & & & X_1^{-1} \end{pmatrix} \right.
$$

$$
\left. \begin{pmatrix} 1 & & & \\ & 1 & & \\ & & 1 & \\ & & 1 & 1 \end{pmatrix} X_3^{+\frac{1}{4}} \begin{pmatrix} 1 & & & \\ & 1 & & \\ & 1 & 1 & \\ & & & X_3^{-1} \end{pmatrix} \begin{pmatrix} 1 & & & \\ & 1 & & \\ & & 1 & \\ & & 1 & 1 \end{pmatrix} Z_1^{''-\frac{1}{4}} Z_2^{''-\frac{2}{4}} Z_3^{''-\frac{3}{4}} \begin{pmatrix} Z_1'' Z_2'' Z_3'' & & & \\ & Z_2'' Z_3'' & & \\ & & Z_3'' & \\ & & & 1 \end{pmatrix} \right].
$$

[Theorem 2.8](#) says that these two matrices are elements of $\mathrm{SL}_4^q(\mathcal{T}_4^\omega)$. For instance, the entries a, b, c, and d of the 2×2 submatrix (arranged as a 4×1 matrix) of $\boldsymbol{L}^\omega$

$$
\begin{pmatrix} a \\ b \\ c \\ d \end{pmatrix} = \begin{pmatrix} \boldsymbol{L}_{13}^\omega \\ \boldsymbol{L}_{14}^\omega \\ \boldsymbol{L}_{23}^\omega \\ \boldsymbol{L}_{24}^\omega \end{pmatrix} = \begin{pmatrix} [Z_3^{\frac{1}{4}} Z_2^{\frac{2}{4}} Z_1^{\frac{3}{4}} Z_3'^{\frac{1}{4}} Z_2'^{-\frac{2}{4}} Z_1'^{-\frac{1}{4}} X_1^{-\frac{1}{4}} X_2^{-\frac{2}{4}} X_3^{-\frac{1}{4}}] + [Z_3^{\frac{1}{4}} Z_2^{\frac{2}{4}} Z_1^{\frac{3}{4}} Z_3'^{\frac{1}{4}} Z_2'^{-\frac{2}{4}} Z_1'^{-\frac{1}{4}} X_1^{-\frac{1}{4}} X_2^{\frac{3}{4}} X_3^{-\frac{1}{4}}] \\ + [Z_3^{\frac{1}{4}} Z_2^{\frac{2}{4}} Z_1^{\frac{3}{4}} Z_3'^{\frac{1}{4}} Z_2'^{-\frac{2}{4}} Z_1'^{-\frac{1}{4}} X_1^{\frac{3}{4}} X_2^{\frac{3}{4}} X_3^{-\frac{1}{4}}] \\ [Z_3^{\frac{1}{4}} Z_2^{\frac{2}{4}} Z_1^{\frac{3}{4}} Z_3'^{-\frac{3}{4}} Z_2'^{-\frac{2}{4}} Z_1'^{-\frac{1}{4}} X_1^{-\frac{1}{4}} X_2^{-\frac{2}{4}} X_3^{-\frac{1}{4}}] \\ [Z_3^{\frac{1}{4}} Z_2^{\frac{2}{4}} Z_1^{-\frac{1}{4}} Z_3'^{\frac{1}{4}} Z_2'^{-\frac{2}{4}} Z_1'^{-\frac{1}{4}} X_1^{-\frac{1}{4}} X_2^{-\frac{2}{4}} X_3^{-\frac{1}{4}}] + [Z_3^{\frac{1}{4}} Z_2^{\frac{2}{4}} Z_1^{-\frac{1}{4}} Z_3'^{\frac{1}{4}} Z_2'^{-\frac{2}{4}} Z_1'^{-\frac{1}{4}} X_1^{-\frac{1}{4}} X_2^{\frac{3}{4}} X_3^{-\frac{1}{4}}] \\ [Z_3^{\frac{1}{4}} Z_2^{\frac{2}{4}} Z_1^{-\frac{1}{4}} Z_3'^{-\frac{3}{4}} Z_2'^{-\frac{2}{4}} Z_1'^{-\frac{1}{4}} X_1^{-\frac{1}{4}} X_2^{-\frac{2}{4}} X_3^{-\frac{1}{4}}] \end{pmatrix}
$$

satisfy ($**$). For a computer demonstration of this see [6, Appendix B]. We also verify in that appendix that ($**$) is satisfied by the entries a, b, c, and d of the 2×2 submatrix (arranged as a 4×1 matrix) of $\boldsymbol{R}^\omega$:

$$
\begin{pmatrix} a \\ b \\ c \\ d \end{pmatrix} = \begin{pmatrix} \boldsymbol{R}_{31}^\omega \\ \boldsymbol{R}_{32}^\omega \\ \boldsymbol{R}_{41}^\omega \\ \boldsymbol{R}_{42}^\omega \end{pmatrix} = \begin{pmatrix} [Z_3^{\frac{1}{4}} Z_2^{-\frac{1}{2}} Z_1^{-\frac{1}{4}} X_2^{\frac{1}{4}} X_1^{\frac{1}{2}} X_3^{\frac{1}{4}} Z_3''^{\frac{1}{4}} Z_2''^{\frac{1}{2}} Z_1''^{\frac{3}{4}}] \\ [Z_3^{\frac{1}{4}} Z_2^{-\frac{1}{2}} Z_1^{-\frac{1}{4}} X_2^{\frac{1}{4}} X_1^{-\frac{1}{2}} X_3^{\frac{1}{4}} Z_3''^{\frac{1}{4}} Z_2''^{\frac{1}{2}} Z_1''^{-\frac{1}{4}}] + [Z_3^{\frac{1}{4}} Z_2^{-\frac{1}{2}} Z_1^{-\frac{1}{4}} X_2^{\frac{1}{4}} X_1^{\frac{1}{2}} X_3^{\frac{1}{4}} Z_3''^{\frac{1}{4}} Z_2''^{\frac{1}{2}} Z_1''^{-\frac{1}{4}}] \\ [Z_3^{-\frac{3}{4}} Z_2^{-\frac{1}{2}} Z_1^{-\frac{1}{4}} X_2^{\frac{1}{4}} X_1^{\frac{1}{2}} X_3^{\frac{1}{4}} Z_3''^{\frac{1}{4}} Z_2''^{\frac{1}{2}} Z_1''^{\frac{3}{4}}] \\ [Z_3^{-\frac{3}{4}} Z_2^{-\frac{1}{2}} Z_1^{-\frac{1}{4}} X_2^{-\frac{3}{4}} X_1^{-\frac{1}{2}} X_3^{\frac{1}{4}} Z_3''^{\frac{1}{4}} Z_2''^{\frac{1}{2}} Z_1''^{-\frac{1}{4}}] \\ + [Z_3^{-\frac{3}{4}} Z_2^{-\frac{1}{2}} Z_1^{-\frac{1}{4}} X_2^{\frac{1}{4}} X_1^{-\frac{1}{2}} X_3^{\frac{1}{4}} Z_3''^{\frac{1}{4}} Z_2''^{\frac{1}{2}} Z_1''^{-\frac{1}{4}}] \\ + [Z_3^{-\frac{3}{4}} Z_2^{-\frac{1}{2}} Z_1^{-\frac{1}{4}} X_2^{\frac{1}{4}} X_1^{\frac{1}{2}} X_3^{\frac{1}{4}} Z_3''^{\frac{1}{4}} Z_2''^{\frac{1}{2}} Z_1''^{-\frac{1}{4}}] \end{pmatrix}
$$

Remark 2.9 In order for these matrices to satisfy the relations required just to be in $\mathrm{M}_n^q(\mathcal{T}_n^\omega)$ (let alone $\mathrm{SL}_n^q(\mathcal{T}_n^\omega)$), they have to be normalized by dividing out their determinants. For example, the above matrix $\boldsymbol{L}^\omega$ for $n = 4$ would not satisfy the q–commutation relations required to be a point of $\mathrm{M}_4^q(\mathcal{T}_4^\omega)$ if we had not included the normalizing term $Z_1^{-1/4} Z_2^{-2/4} Z_3^{-3/4} X_1^{-1/4} X_2^{-2/4} X_3^{-1/4} Z_1'^{-1/4} Z_2'^{-2/4} Z_3'^{-3/4}$, as there would be a 1 in the bottom corner.

3 Quantum snakes: proof of [Theorem 2.8](#)

Above, we gave a sketch of the proof. We now fill in the details. Our emphasis will be on the left matrix $\boldsymbol{L}^\omega$. The proof for the right matrix $\boldsymbol{R}^\omega$ is similar, as we will discuss in [Section 3.5](#).
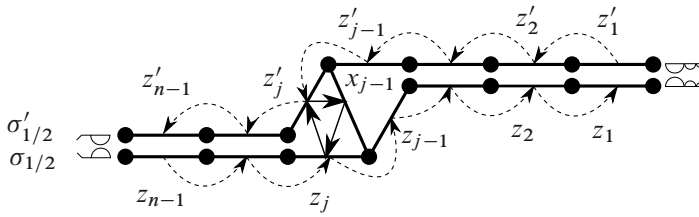
Figure 13: Diamond snake-move algebra for $j = 2, \ldots, n-1$.

Fix a sequence $\sigma^{\mathrm{bot}} = \sigma^1, \sigma^2, \ldots, \sigma^N = \sigma^{\mathrm{top}}$ of adjacent snakes, as in the left setting; see Section 1.4.1. The proof is valid for any choice of snake sequence, but our demonstrations in figures and examples will be for our preferred snake sequence; see Figure 8. Note that the example quantum matrices in Section 2.5 were presented using this preferred snake sequence.

3.1 Snake-move quantum tori

Definition 3.1 For $j = 1, \ldots, n-1$, the jth *snake-move quantum torus* $\mathcal{S}_j^\omega = \mathcal{T}(\boldsymbol{P}_j)$ is the quantum torus with Poisson matrix $\boldsymbol{P}_j$ defined by the quiver shown in Figure 13 when $j = 2, \ldots, n-1$, and in Figure 14 when $j = 1$. As usual, there is one generator per edge of the quiver, solid arrows carry a weight 2, and dotted arrows carry a weight 1; compare with Section 2.2.

Conceptual Remark 3.2 We provide some guiding intuition for the upcoming constructions; strictly speaking, it is not required for the mathematical progression of the article.

The quiver of Figure 14 for the tail-move quantum torus is divided into a bottom and top side. Similarly, the quiver of Figure 13 for a diamond-move quantum torus has a bottom and top side, connected by a diagonal (where the variable x_{j-1} is located). As illustrated in the figures, we think of the bottom side (with unprimed generators z_j) as the top "snake-half" $\sigma_{1/2}$ of a snake σ that has been "split in half down its length". Similarly, we think of the top side (with primed generators z_j') as the bottom snake-half $\sigma_{1/2}'$ of a split snake σ'. Compare with Figure 3, which illustrates a classical snake "before splitting".

This snake splitting can be seen more clearly in the *quantum snake sweep* (see Section 3.3 and Figure 15) determined by the sequence of adjacent snakes $\sigma^{\mathrm{bot}} = \sigma^1, \sigma^2, \ldots, \sigma^N = \sigma^{\mathrm{top}}$, where each snake σ^i is split in half, so that each snake-half forms a side in one of two adjacent snake-move quantum tori. In the figure, the other halves (colored gray) of the bottom-most and top-most quantum snakes can be thought of as either living in other triangles or not existing at all. Prior to splitting a snake σ in half, the snake
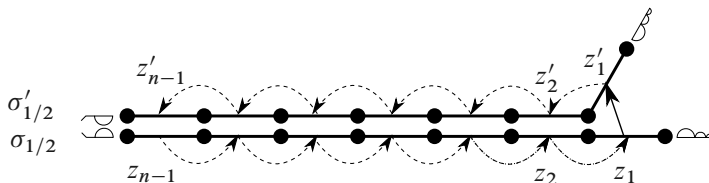
Figure 14: Tail snake-move algebra for $j = 1$.

consists of $n-1$ "vertebrae" connecting the n snake-vertices $\sigma_k \in \Theta_{n-1}$. Upon splitting the snake, the jth vertebra splits into two generators z_j and z'_j living in adjacent snake-move quantum tori.

3.2 Quantum snake-move matrices

We turn to the key observation for the proof.

Proposition 3.3 *For $j = 1, \ldots, n-1$, the jth quantum snake-move matrix*

$$M_j := \left[\left(\prod_{k=1}^{n-1} S_k^{\text{edge}}(z_k) \right) S_j^{\text{left}}(x_{j-1}) \left(\prod_{k=1}^{n-1} S_k^{\text{edge}}(z'_k) \right) \right] \in M_n(\mathcal{S}_j^{\omega})$$

is an $\mathcal{S}_j^{\omega}$–point of the quantum special linear group SL_n^q. That is, $M_j \in \text{SL}_n^q(\mathcal{S}_j^{\omega}) \subseteq M_n(\mathcal{S}_j^{\omega})$.

Note the use of the Weyl quantum ordering; see Section 2.1.3. Here the matrices $S_k^{\text{edge}}(z)$ and $S_j^{\text{left}}(x)$ for z and x in the commutative algebra $\mathcal{S}_j^1$ are defined as in Section 1.3.1; see also Sections 2.3.1 and 2.3.2. When $j = 1$, the matrix $S_1^{\text{left}}(x_0) = S_1^{\text{left}}$ is well defined, despite x_0 not being defined.

Proposition 3.3 follows from direct calculation. See Section 3.5 for the proof.

For example, in the case $n = 4$ and $j = 3$, the lemma says that the matrix

$$M_3 = \left[z_1^{-\frac{1}{4}} z_2^{-\frac{2}{4}} z_3^{-\frac{3}{4}} \begin{pmatrix} z_1 z_2 z_3 & & & \\ & z_2 z_3 & & \\ & & z_3 & \\ & & & 1 \end{pmatrix} x_2^{-\frac{2}{4}} \begin{pmatrix} x_2 & & & \\ & x_2 & & \\ & & 1 & 1 \\ & & & 1 \end{pmatrix} z_1'^{-\frac{1}{4}} z_2'^{-\frac{2}{4}} z_3'^{-\frac{3}{4}} \begin{pmatrix} z_1' z_2' z_3' & & & \\ & z_2' z_3' & & \\ & & z_3' & \\ & & & 1 \end{pmatrix} \right]$$

is in $\text{SL}_4^q(\mathcal{S}_3^{\omega})$.

3.3 Technical step: embedding a distinguished subalgebra $\mathcal{T}_L$ of $\mathcal{T}_n^{\omega}$ into a tensor product $\bigotimes_{i=1}^{N-1} \mathcal{S}_{j_i}^{\omega}$ of snake-move quantum tori

For the snake-sequence $(\sigma^i)_{i=1,\ldots,N}$, to each pair (σ^i, σ^{i+1}) of adjacent snakes we associate a snake-move quantum torus $\mathcal{S}_{j_i}^{\omega}$, recalling Figure 15 (see also Conceptual Remark 3.2). Here j_i corresponds to what was called k in Definition 1.7. Recall the Fock–Goncharov quantum torus $\mathcal{T}_n^{\omega}$ (for example, Figure 12).

We now take a technical step. Using the notation of Figures 11 and 12, define $\mathcal{T}_L \subseteq \mathcal{T}_n^{\omega}$ ("L" for "left") to be the subalgebra generated by all the generators (and their inverses) of $\mathcal{T}_n^{\omega}$ except for $Z_1''^{\pm 1/n}, \ldots, Z_{n-1}''^{\pm 1/n}$. We claim that the snake-sequence $(\sigma^i)_i$ induces an embedding

$$\mathcal{T}_L \xrightarrow{(\sigma^i)_i} \bigotimes_{i=1}^{N-1} \mathcal{S}_{j_i}^{\omega}$$

of algebras, realizing $\mathcal{T}_L \subseteq \mathcal{T}_n^{\omega}$ as a subalgebra of the tensor product of the snake-move quantum tori $\mathcal{S}_{j_i}^{\omega}$ associated to the adjacent snake pairs (σ^i, σ^{i+1}). Here recall in general that the algebra structure for a tensor product $A \otimes B$ of algebras A and B is defined by $(a \otimes b) \cdot (a' \otimes b') = (a \cdot a') \otimes (b \cdot b')$ for all $a, a' \in A$ and $b, b' \in B$, extended linearly.
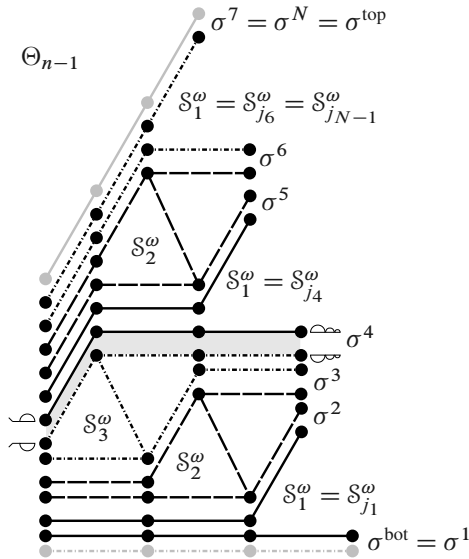
Figure 15: Quantum snake sweep for $n = 4$; compare with Figure 8, left.

A more formal definition of the embedding will be given in Section 3.3.1. We first explain the embedding through an example, in the setting $n = 4$; see Figure 16 (compare with Figure 15).

In this setting, the coordinate X_2, for instance (emphasized in Figure 16), is mapped via

$$X_2 \mapsto 1 \otimes z_2' \otimes z_2 x_2 z_2' \otimes z_2 z_2' \otimes z_2 \otimes 1 \in \mathcal{S}_1^\omega \otimes \mathcal{S}_2^\omega \otimes \mathcal{S}_3^\omega \otimes \mathcal{S}_1^\omega \otimes \mathcal{S}_2^\omega \otimes \mathcal{S}_1^\omega.$$

Similarly, the other coordinates Z_1, Z_3', Z_2, Z_3, X_1, X_1', Z_2', and Z_1' are mapped via

$$Z_1 \mapsto z_1 \otimes 1 \otimes 1 \otimes 1 \otimes 1 \otimes 1, \qquad\qquad Z_3' \mapsto 1 \otimes 1 \otimes z_3' \otimes z_3 z_3' \otimes z_3 z_3' \otimes z_3 z_3',$$

$$Z_2 \mapsto z_2 z_2' \otimes z_2 \otimes 1 \otimes 1 \otimes 1 \otimes 1, \qquad\quad Z_3 \mapsto z_3 z_3' \otimes z_3 z_3' \otimes z_3 \otimes 1 \otimes 1 \otimes 1,$$

$$X_1 \mapsto z_1' \otimes z_1 x_1 z_1' \otimes z_1 z_1' \otimes z_1 \otimes 1 \otimes 1, \quad X_1' \mapsto 1 \otimes 1 \otimes 1 \otimes z_1' \otimes z_1 x_1 z_1' \otimes z_1,$$

$$Z_2' \mapsto 1 \otimes 1 \otimes 1 \otimes 1 \otimes z_2' \otimes z_2 z_2', \qquad\qquad Z_1' \mapsto 1 \otimes 1 \otimes 1 \otimes 1 \otimes 1 \otimes z_1'.$$

Note that the monomials (for instance, $z_2 x_2 z_2'$ or $z_2 z_2'$) appearing in the ith tensor factor of the image of a generator X or Z of the subalgebra $\mathcal{T}_L$ under this mapping consist of mutually commuting generators x's and/or z's of the ith snake-move quantum torus $\mathcal{S}_{j_i}^\omega$, so the order in which they are written is irrelevant. It is clear from Figure 16 that these images satisfy the relations of $\mathcal{T}_L$. In particular, the "interior" dotted arrows lying at each interface between two snake-move quantum tori cancel each other out; note that, in Figure 16, we have omitted drawing some of these dotted arrows. We gather that the mapping is well defined and is an algebra homomorphism. Injectivity follows from the property that every generator (that is, quiver edge) appearing on the right side of Figure 16 corresponds to a unique generator on the left side. Lastly, we technically should have defined the map on the formal n–roots of the coordinates of $\mathcal{T}_L$. This is done in the obvious way; for instance,

$$X_2^{\frac{1}{4}} \mapsto 1 \otimes z_2'^{\frac{1}{4}} \otimes z_2^{\frac{1}{4}} x_2^{\frac{1}{4}} z_2'^{\frac{1}{4}} \otimes z_2^{\frac{1}{4}} z_2'^{\frac{1}{4}} \otimes z_2^{\frac{1}{4}} \otimes 1 \in \mathcal{S}_1^\omega \otimes \mathcal{S}_2^\omega \otimes \mathcal{S}_3^\omega \otimes \mathcal{S}_1^\omega \otimes \mathcal{S}_2^\omega \otimes \mathcal{S}_1^\omega.$$
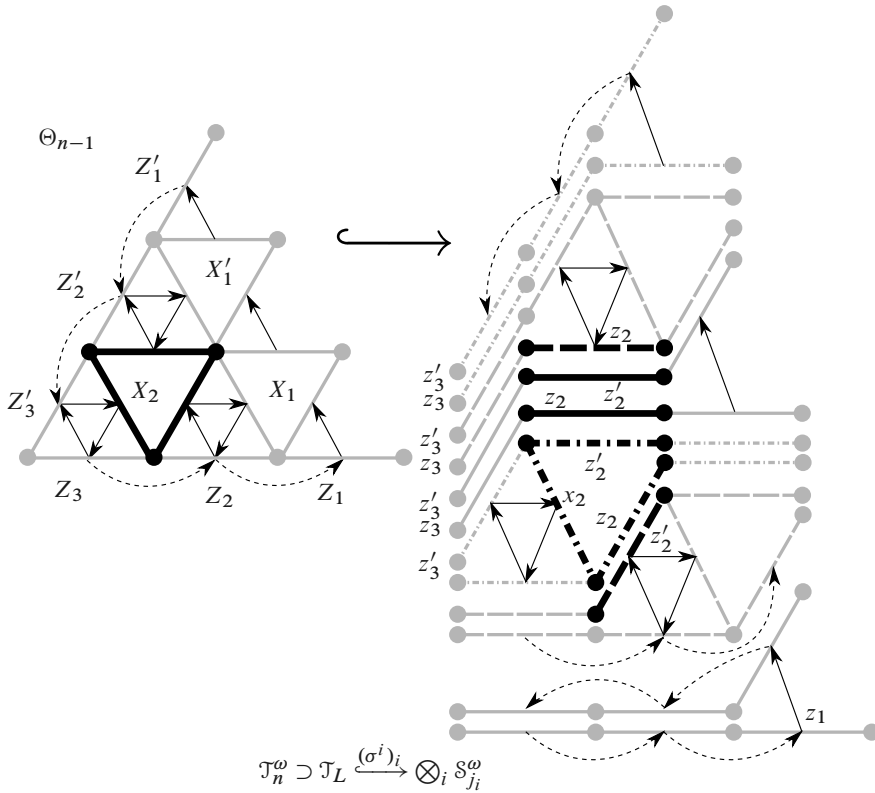
Figure 16: Embedding $\mathcal{T}_L$ in the tensor product of snake-move quantum tori.

3.3.1 Formal definition of the embedding A *segment* $\overline{\mu\nu} = \overline{\nu\mu}$ of the discrete triangle Θ_{n-1} is a line connecting neighboring vertices μ and ν. Segments of the form $\overline{(\alpha, \beta, \gamma), (\alpha-1, \beta, \gamma+1)}$ are called *horizontal*, segments of the form $\overline{(\alpha, \beta, \gamma), (\alpha-1, \beta+1, \gamma)}$ are called *acute*, and segments of the form $\overline{(\alpha, \beta, \gamma), (\alpha, \beta+1, \gamma-1)}$ are called *obtuse*. Let Seg_L denote the set of segments minus the obtuse segments with zero first coordinate. For example, in the case $n = 4$, the set Seg_L has 15 elements; see the left-hand side of Figure 16. Let $\mathrm{Coord}_L \subseteq \mathcal{T}_L$ denote the set of coordinates, that is,

$$\mathrm{Coord}_L = \{X_{abc} \mid (a, b, c) \in \mathrm{int}(\Theta_n)\} \cup \{Z_j \mid j = 1, 2, \ldots, n-1\} \cup \{Z_j' \mid j = 1, 2, \ldots, n-1\}.$$

Note that the coordinates X_{abc} correspond to the small downward facing triangles in Θ_{n-1}, each of which is a union of a horizontal, acute, and obtuse segment in Seg_L, the coordinates Z_j correspond to horizontal segments with zero second coordinate, the coordinates Z_j' correspond to acute segments with zero third coordinate, and each segment corresponds in this way to a unique coordinate. In particular, there is a canonical surjective function $\pi' \colon \mathrm{Seg}_L \to \mathrm{Coord}_L \subseteq \mathcal{T}_L$. See the left-hand side of Figure 16 for the case $n = 4$, where for example the three bold segments constitute the preimage $\pi'^{-1}(X_2)$.

Given a snake sequence $(\sigma^i)_{i=1,2,\ldots,N}$, for each $1 \leqslant i \leqslant N-1$ let $\mathrm{Coord}^i \subseteq \mathcal{S}_{j_i}^\omega$ denote the set of coordinates in the snake-move quantum torus $\mathcal{S}_{j_i}^\omega$. There are associated functions $\varphi^i \colon \mathrm{Coord}^i \to \mathrm{Coord}_L$, in general neither surjective nor injective, defined as follows. To each coordinate $z_k \in \mathcal{S}_{j_i}^\omega$ for $k = 1, 2, \ldots, n-1$ there

is associated a segment $\mathrm{seg}(z_k) \in \mathrm{Seg}_L$ of the snake σ^i, namely $\mathrm{seg}(z_k) = \overline{\sigma^i_{k+1}\sigma^i_k}$, to each coordinate $z'_k \in S^\omega_{j_i}$ for $k = 1, 2, \ldots, n-1$ there is associated a segment $\mathrm{seg}(z'_k) \in \mathrm{Seg}_L$ of the snake σ^{i+1}, namely $\mathrm{seg}(z'_k) = \overline{\sigma^{i+1}_{k+1}\sigma^{i+1}_k}$, and to the coordinate $x_{j_i-1} \in S^\omega_{j_i}$ there is associated an obtuse segment $\mathrm{seg}(x_{j_i-1}) \in \mathrm{Seg}_L$ which is not a segment of a snake, namely $\mathrm{seg}(x_{j_i-1}) = \overline{\sigma^i_{j_i}\sigma^{i+1}_{j_i}}$. Compare with Figure 15. Then φ^i is defined by $\varphi^i(x) = \pi'(\mathrm{seg}(x))$ for all $x \in \mathrm{Coord}^i$.

For example in the case $n = 4$, as illustrated in Figure 16, we have $\varphi^1(z_1) = Z_1$, $\varphi^2(z'_2) = X_2$, $\varphi^3(x_2) = X_2$, $\varphi^4(z'_2) = X_2$, $\varphi^5(z_2) = X_2$, and $\varphi^6(z_3) = Z'_3$.

Finally, define the desired embedding on generators $X^{1/n}$ of $\mathcal{T}_L$, for $X \in \mathrm{Coord}_L$, so that the image of $X^{1/n}$ in the tensor product $\bigotimes_i S^\omega_{j_i}$ is the pure tensor defined by the property that its ith factor is $\prod_{x \in (\varphi^i)^{-1}(X)} x^{1/n} \in S^\omega_{j_i}$. This is well defined since the coordinates $x \in (\varphi^i)^{-1}(X)$ in each preimage commute by design. Note, by definition, if $(\varphi^i)^{-1}(X)$ is empty, then the product defining the ith factor is 1.

In Section 3.4, we will make use of the surjective function $\pi \colon \bigcup_{i=1}^{N-1} \mathrm{Coord}^i \to \mathrm{Coord}_L$ defined by $\pi(x) = \varphi^i(x)$ for $x \in \mathrm{Coord}^i$.

3.4 Finishing the proof

Comparing to the sketch of proof given in Section 2.4.2, we gather:

- $M_{\mathrm{FG}} := L^\omega \in \mathrm{M}_n(\mathcal{T}_L) \subseteq \mathrm{M}_n\big(\bigotimes_{i=1}^{N-1} S^\omega_{j_i}\big)$.
- $M := M_{j_1} M_{j_2} \cdots M_{j_{N-1}} \in \mathrm{SL}^q_n\big(\bigotimes_{i=1}^{N-1} S^\omega_{j_i}\big) \subseteq \mathrm{M}_n\big(\bigotimes_{i=1}^{N-1} S^\omega_{j_i}\big)$.

To finish the proof, it remains to show

$$(*\!*\!*) \qquad\qquad M_{\mathrm{FG}} \overset{?}{=} M \in \mathrm{M}_n\left(\bigotimes_{i=1}^{N-1} S^\omega_{j_i}\right).$$

The strategy is to commute the many variables (as in the right-hand side of Figure 16) appearing on the right-hand side $M = \prod_i M_{j_i}$ (defined via Proposition 3.3) of $(*\!*\!*)$, until M has been put into the form of the left-hand side M_{FG} (defined via Definition 2.4 followed by applying the embedding $\mathcal{T}_L \hookrightarrow \bigotimes_i S^\omega_{j_i}$ of Section 3.3). This is accomplished by applying the following two facts:

Lemma 3.4 (1) *If $\tilde{M}_1, \tilde{M}_2, \ldots, \tilde{M}_{N-1}$ are $n \times n$ matrices with coefficients in $(q = \omega = \omega^{1/2} = 1)$– specializations $\mathcal{T}^1_i$ of general quantum tori $\mathcal{T}^\omega_1, \mathcal{T}^\omega_2, \ldots, \mathcal{T}^\omega_{N-1}$, viewed as factors in*

$$\mathcal{T}^\omega_1 \otimes \mathcal{T}^\omega_2 \otimes \cdots \otimes \mathcal{T}^\omega_{N-1},$$

then

$$[\tilde{M}_1][\tilde{M}_2]\cdots[\tilde{M}_{N-1}] = [\tilde{M}_1 \tilde{M}_2 \cdots \tilde{M}_{N-1}] \in \mathrm{M}_n(\mathcal{T}^\omega_1 \otimes \mathcal{T}^\omega_2 \otimes \cdots \otimes \mathcal{T}^\omega_{N-1}).$$

Here we are viewing the tensor product $\mathcal{T}^\omega_1 \otimes \mathcal{T}^\omega_2 \otimes \cdots \otimes \mathcal{T}^\omega_{N-1}$ as a quantum torus in the obvious way, as demonstrated in the proof below.

(2) *For commuting variables z and x, the matrices $S^{\mathrm{edge}}_k(z)$ and $S^{\mathrm{left}}_j(x)$, as in Section 1.3.1, satisfy*

$$S^{\mathrm{edge}}_k(z) S^{\mathrm{left}}_j(x) = S^{\mathrm{left}}_j(x) S^{\mathrm{edge}}_k(z) \ \text{ if and only if } \ k \neq j.$$

Proof The proof of (1) is straightforward. To simplify the notation, we demonstrate the calculation for two matrices $\widetilde{M}$ and $\widetilde{N}$ with coefficients in classical tori $\mathcal{T}$ and $\mathcal{U}$ with coordinates $\{X_i\}_{i=1,2,\dots,m}$ and $\{Y_j\}_{j=1,2,\dots,p}$ and quivers ϵ and ζ, respectively, where $\mathcal{T}$ and $\mathcal{U}$ are viewed in $\mathcal{T} \otimes \mathcal{U}$. The proof for finitely many matrices is analogous.

By linearity, it suffices to assume $\widetilde{M}_{ij} \in \mathcal{T}$ and $\widetilde{N}_{kl} \in \mathcal{U}$ are monomials, that is,

$$\widetilde{M}_{ij} = X_1^{a_1^{ij}} X_2^{a_2^{ij}} \cdots X_m^{a_m^{ij}} \quad \text{and} \quad \widetilde{N}_{kl} = Y_1^{b_1^{kl}} Y_2^{b_2^{kl}} \cdots Y_p^{b_p^{kl}}.$$

Recall that, by definition, different tensor factors commute under multiplication in $\mathcal{T} \otimes \mathcal{U}$. We have, for all $1 \leq i, j \leq n$,

$$
\begin{aligned}
[\widetilde{M}\widetilde{N}]_{ij} = [(\widetilde{M}\widetilde{N})_{ij}] &= \sum_k [\widetilde{M}_{ik}\widetilde{N}_{kj}] = \sum_k [X_1^{a_1^{ik}} X_2^{a_2^{ik}} \cdots X_m^{a_m^{ik}} Y_1^{b_1^{kj}} Y_2^{b_2^{kj}} \cdots Y_p^{b_p^{kj}}] \\
&= \sum_k q^{-\frac{1}{2}\kappa} X_1^{a_1^{ik}} X_2^{a_2^{ik}} \cdots X_m^{a_m^{ik}} Y_1^{b_1^{kj}} Y_2^{b_2^{kj}} \cdots Y_p^{b_p^{kj}} \\
&= \sum_k q^{-\frac{1}{2}\xi} X_1^{a_1^{ik}} X_2^{a_2^{ik}} \cdots X_m^{a_m^{ik}} Y_1^{b_1^{kj}} Y_2^{b_2^{kj}} \cdots Y_p^{b_p^{kj}} \\
&= \sum_k [X_1^{a_1^{ik}} X_2^{a_2^{ik}} \cdots X_m^{a_m^{ik}}][Y_1^{b_1^{kj}} Y_2^{b_2^{kj}} \cdots Y_p^{b_p^{kj}}] = \sum_k [\widetilde{M}_{ik}][\widetilde{N}_{kj}] = ([\widetilde{M}][\widetilde{N}])_{ij},
\end{aligned}
$$

where

$$\kappa = \sum_{1 \leq \alpha < \beta \leq m} (\epsilon \otimes \zeta)_{\alpha\beta} a_\alpha^{ik} a_\beta^{ik} + \sum_{1 \leq \alpha \leq m, 1 \leq \beta \leq p} (\epsilon \otimes \zeta)_{\alpha(m+\beta)} a_\alpha^{ik} b_\beta^{kj} + \sum_{1 \leq \alpha < \beta \leq p} (\epsilon \otimes \zeta)_{(m+\alpha)(m+\beta)} b_\alpha^{kj} b_\beta^{kj}$$

and

$$\xi = \sum_{1 \leq \alpha < \beta \leq m} \epsilon_{\alpha\beta} a_\alpha^{ik} a_\beta^{ik} + \sum_{1 \leq \alpha \leq m, 1 \leq \beta \leq p} 0 a_\alpha^{ik} b_\beta^{kj} + \sum_{1 \leq \alpha < \beta \leq p} \zeta_{\alpha\beta} b_\alpha^{kj} b_\beta^{kj}.$$

The proof of (2) is by inspection.   □

Proof of Theorem 2.8 By Lemma 3.4(1), it suffices to establish $(***)$ when $q = \omega = \omega^{1/2} = 1$, in which case we do not need to worry about the Weyl quantum ordering.

It is helpful to introduce a simplifying notation. For coordinates $z_k^{(i)}, x_j^{(i)}, z_k'^{(i)} \in \mathcal{S}_{j_i}^1$, put

$$\boldsymbol{Z}_k^{(i)} := \boldsymbol{S}_k^{\text{edge}}(z_k^{(i)}), \quad \boldsymbol{X}_j^{(i)} := \boldsymbol{S}_{j+1}^{\text{left}}(x_j^{(i)}), \quad \text{and} \quad \boldsymbol{Z}_k'^{(i)} := \boldsymbol{S}_k^{\text{edge}}(z_k'^{(i)}) \in \mathrm{M}_n(\mathcal{S}_{j_i}^1).$$

In this new notation, the matrices $\boldsymbol{M}_{j_i} \in \mathrm{M}_n(\mathcal{S}_{j_i}^1)$ of Proposition 3.3 can be expressed by

$$\boldsymbol{M}_{j_i} = \left(\prod_{k=1}^{n-1} \boldsymbol{Z}_k^{(i)}\right) \boldsymbol{X}_{j_i-1}^{(i)} \left(\prod_{k=1}^{n-1} \boldsymbol{Z}_k'^{(i)}\right) \in \mathrm{M}_n(\mathcal{S}_{j_i}^1),$$

and Lemma 3.4(2) now reads, for any $i_1, i_2 \in \{1, 2, \dots, N-1\}$,

$$(\dagger) \quad \boldsymbol{Z}_k^{(i_1)} \boldsymbol{X}_j^{(i_2)} = \boldsymbol{X}_j^{(i_2)} \boldsymbol{Z}_k^{(i_1)} \in \mathrm{M}_n\left(\bigotimes_{i=1}^{N-1} \mathcal{S}_{j_i}^1\right) \quad \text{if and only if} \quad k \neq j+1 \quad \text{(similarly for } \boldsymbol{Z} \to \boldsymbol{Z}').$$

Example ($n = 2$) In this case, $N = 2$, we have $\mathcal{S}^1_{j_1} = \mathcal{S}^1_1 \cong \mathcal{T}_L \subseteq \mathcal{T}^1_n$, and the embedding $\mathcal{T}_L \hookrightarrow \mathcal{S}^1_1$ is the identity, where $Z_1 \mapsto z^{(1)}_1$ and $Z'_1 \mapsto z'^{(1)}_1$. Equation ($***$) is also trivial, reading

$$M = M_1 = \boldsymbol{Z}^{(1)}_1 \boldsymbol{X}^{(1)}_0 \boldsymbol{Z}'^{(1)}_1 = z^{(1)\frac{-1}{2}}_1 \begin{pmatrix} z^{(1)}_1 & 0 \\ 0 & 1 \end{pmatrix} \begin{pmatrix} 1 & 1 \\ 0 & 1 \end{pmatrix} z'^{(1)\frac{-1}{2}}_1 \begin{pmatrix} z'^{(1)}_1 & 0 \\ 0 & 1 \end{pmatrix}$$

$$= Z^{-\frac{1}{2}}_1 \begin{pmatrix} Z_1 & 0 \\ 0 & 1 \end{pmatrix} \begin{pmatrix} 1 & 1 \\ 0 & 1 \end{pmatrix} Z'^{-\frac{1}{2}}_1 \begin{pmatrix} Z'_1 & 0 \\ 0 & 1 \end{pmatrix} = \boldsymbol{S}^{\mathrm{edge}}_1(Z_1)\boldsymbol{S}^{\mathrm{left}}_1 \boldsymbol{S}^{\mathrm{edge}}_1(Z'_1) = \boldsymbol{M}_{\mathrm{FG}}.$$

Example ($n = 3$) Here $N = 4$, the subalgebra $\mathcal{T}_L$ has coordinates Z_1, Z_2, X_1, Z'_1 and Z'_2, and the embedding $\mathcal{T}_L \hookrightarrow \mathcal{S}^1_1 \otimes \mathcal{S}^1_2 \otimes \mathcal{S}^1_1$ is defined by (compare the $n = 4$ case, Figure 16)

$$Z_1 \mapsto z^{(1)}_1, \quad Z_2 \mapsto z^{(1)}_2 z'^{(1)}_2 z^{(2)}_2, \quad X_1 \mapsto z'^{(1)}_1 z^{(2)}_1 x^{(2)}_1 z'^{(2)}_1 z^{(3)}_1, \quad Z'_1 \mapsto z'^{(3)}_1, \quad \text{and} \quad Z'_2 \mapsto z'^{(2)}_2 z^{(3)}_2 z'^{(3)}_2,$$

where we have suppressed the tensor products. Note in this case there is a unique snake-sequence $(\sigma^i)_{i=1,\dots,4}$ so there is only one associated embedding of $\mathcal{T}_L$. Equation ($***$) reads

$$M = M_1 M_2 M_1 = \underline{\boldsymbol{Z}}^{(1)}_1 \underline{\boldsymbol{Z}}^{(1)}_2 \underline{\boldsymbol{X}}^{(1)}_0 \boldsymbol{Z}'^{(1)}_1 \boldsymbol{Z}'^{(1)}_2 \cdot \boldsymbol{Z}^{(2)}_1 \boldsymbol{Z}^{(2)}_2 \underline{\boldsymbol{X}}^{(2)}_1 \boldsymbol{Z}'^{(2)}_1 \boldsymbol{Z}'^{(2)}_2 \cdot \boldsymbol{Z}^{(3)}_1 \boldsymbol{Z}^{(3)}_2 \underline{\boldsymbol{X}}^{(3)}_0 \underline{\boldsymbol{Z}}'^{(3)}_1 \underline{\boldsymbol{Z}}'^{(3)}_2$$

$$= \underline{\boldsymbol{Z}}^{(1)}_1 \cdot \underline{\boldsymbol{Z}}^{(1)}_2 \boldsymbol{Z}'^{(1)}_2 \boldsymbol{Z}^{(2)}_2 \cdot \underline{\boldsymbol{X}}^{(1)}_0 \cdot \boldsymbol{Z}'^{(1)}_1 \boldsymbol{Z}^{(2)}_1 \underline{\boldsymbol{X}}^{(2)}_1 \boldsymbol{Z}'^{(2)}_1 \boldsymbol{Z}^{(3)}_1 \cdot \underline{\boldsymbol{X}}^{(3)}_0 \cdot \underline{\boldsymbol{Z}}'^{(3)}_1 \cdot \boldsymbol{Z}'^{(2)}_2 \boldsymbol{Z}^{(3)}_2 \underline{\boldsymbol{Z}}'^{(3)}_2$$

$$= \boldsymbol{S}^{\mathrm{edge}}_1(Z_1)\boldsymbol{S}^{\mathrm{edge}}_2(Z_2)\boldsymbol{S}^{\mathrm{left}}_1 \boldsymbol{S}^{\mathrm{left}}_2(X_1)\boldsymbol{S}^{\mathrm{left}}_1 \boldsymbol{S}^{\mathrm{edge}}_1(Z'_1)\boldsymbol{S}^{\mathrm{edge}}_2(Z'_2) = \boldsymbol{M}_{\mathrm{FG}},$$

where for the third equality we have used the reformulation (†) of Lemma 3.4(2) to commute the matrices. Note that the ordering of terms in any of the seven groupings in the fourth expression is immaterial. The fourth equality uses the embedding $\mathcal{T}_L \hookrightarrow \mathcal{S}^1_1 \otimes \mathcal{S}^1_2 \otimes \mathcal{S}^1_1$.

General case As we saw in the examples, $M = \prod^{N-1}_{i=1} M_{j_i}$ is a product of distinct terms $\boldsymbol{Z}^{(i)}_k$, $\boldsymbol{X}^{(i)}_j$, or $\boldsymbol{Z}'^{(i)}_k$. Let A be the set of terms, that is, $A = \bigcup_{i=1,2,\dots,N-1}\{\boldsymbol{Z}^{(i)}_k, \boldsymbol{X}^{(i)}_{j_i-1}, \boldsymbol{Z}'^{(i)}_k \mid k = 1, 2, \dots, n-1\}$. Besides terms of the form $\boldsymbol{X}^{(i)}_0$, there is one term in A for each coordinate $z^{(i)}_k$, $x^{(i)}_j$, and $z'^{(i)}_k$ of $\bigotimes^{N-1}_{i=1} \mathcal{S}^1_{j_i}$. We show that there is an algorithm that commutes these terms into the correct groupings, as in the above examples.

There is a distinguished subset $A_L \subseteq A$, precisely defined in the next paragraph. In the example $n = 2$, $A_L = A$, and in the example $n = 3$, the terms in A_L are underlined above. All the $\boldsymbol{X}^{(i)}_0$ terms are in A_L. Besides the $\boldsymbol{X}^{(i)}_0$ terms, there is one term in A_L for each coordinate Z_k, X_j, and Z'_k of $\mathcal{T}_L$; see Figure 16. As another example, for $n = 4$ and our usual preferred snake sequence $(\sigma^i)_i$, $A_L = \{\boldsymbol{Z}^{(1)}_1, \boldsymbol{Z}^{(1)}_2, \boldsymbol{Z}^{(1)}_3, \boldsymbol{X}^{(1)}_0, \boldsymbol{X}^{(2)}_1, \boldsymbol{X}^{(3)}_2, \boldsymbol{X}^{(4)}_0, \boldsymbol{X}^{(5)}_1, \boldsymbol{X}^{(6)}_0, \boldsymbol{Z}'^{(6)}_1, \boldsymbol{Z}'^{(6)}_2, \boldsymbol{Z}'^{(6)}_3\}$; see Figures 15 and 16.

More precisely, the general definition of $A_L \subseteq A$, valid for any snake sequence $(\sigma^i)_{i=1,2,\dots,N}$, is as follows. First, $\boldsymbol{Z}^{(1)}_k = \boldsymbol{S}^{\mathrm{edge}}_k(z^{(1)}_k)$, $\boldsymbol{Z}'^{(N-1)}_k = \boldsymbol{S}^{\mathrm{edge}}_k(z'^{(N-1)}_k)$, and $\boldsymbol{X}^{(i)}_0 = \boldsymbol{S}^{\mathrm{left}}_1$ are in A_L for all $k = 1, 2, \dots, n-1$ and for all $1 \leqslant i \leqslant N-1$ such that $j_i - 1 = 0$. And $\boldsymbol{X}^{(i)}_{j_i-1} = \boldsymbol{S}^{\mathrm{left}}_{j_i}(x^{(i)}_{j_i-1})$ is in A_L for all $1 \leqslant i \leqslant N-1$ such that $j_i > 1$.

Recall that the injectivity of the embedding $\mathcal{T}_L \hookrightarrow \bigotimes^{N-1}_{i=1} \mathcal{S}^1_{j_i}$ followed immediately from the property that every coordinate $z^{(i)}_k$, $x^{(i)}_j$, or $z'^{(i)}_k$ of $\bigotimes^{N-1}_{i=1} \mathcal{S}^1_{j_i}$ corresponds to a unique coordinate Z_k, X_j, or Z'_k of $\mathcal{T}_L$;

see Figure 16. This property thus defines a retraction $r: A \twoheadrightarrow A_L$, namely a surjective function restricting to the identity on $A_L \subseteq A$ (by definition, $X_0^{(i)} \mapsto X_0^{(i)}$). See the next paragraph for a precise definition. The retraction r can be visualized as collapsing the right side of Figure 16 to obtain the left side.

More precisely, in the notation of Section 3.3.1, there is a bijection $f: A - A_0 \to \bigcup_{i=1}^{N-1} \mathrm{Coord}^i$ defined by $f(Z_k^{(i)}) = z_k^{(i)}$, $f(Z_k'^{(i)}) = z_k'^{(i)}$, and $f(X_{j_i-1}^{(i)}) = x_{j_i-1}^{(i)}$. Here we have put

$$A_0 = \{X_0^{(i)} \mid 1 \leqslant i \leqslant N - 1 \text{ such that } j_i - 1 = 0\}.$$

By definition of A_L, the restricted composition g defined by $g = \pi \circ (f|_{A_L - A_0}): A_L - A_0 \to \mathrm{Coord}_L$ is a bijection, where $\pi: \bigcup_{i=1}^{N-1} \mathrm{Coord}^i \to \mathrm{Coord}_L$ is defined at the end of Section 3.3.1. The retraction $r: A \to A_L$ is defined on $A - A_0$ by $r = g^{-1} \circ \pi \circ f$, and as the identity on $A_0 \subseteq A_L$.

The desired algorithm grouping the terms in A, where there is one grouping per term in A_L, is defined by selecting an ungrouped term $a \in A$ and commuting it left or right until it is adjacent to $r(a) \in A_L$. Here the terms are viewed in the expression for M. This commutation is possible by Lemma 3.4(2), that is, (†).

More precisely, in the expression for M at step s of the algorithm, for each $a_0 \in A_L$ let $l(a_0, s)$ denote the length of the longest chain of adjacent terms $a \in r^{-1}(a_0)$ such that this chain contains a_0. For instance, in the $n = 3$ example above, for $a_0 = X_1^{(2)}$, initially the length of the chain containing a_0 is 2, while at the end of the algorithm this length is $5 = |r^{-1}(a_0)|$. Assuming for the moment that the algorithm is well defined, that is, that the commutation is possible, we see that $l(a_0, s) \leqslant l(a_0, s+1)$ for all $a_0 \in A_L$ and for all steps s, and moreover that at least one of these inequalities is strict at each step. It follows that the algorithm terminates, at which point the length $l(a_0, s_{\mathrm{term}})$ of the chain containing a_0 is $|r^{-1}(a_0)|$ for all $a_0 \in A_L$. Thus in the expression for M at the end of the algorithm, replacing each string $\prod_{a \in r^{-1}(a_0)} a$ with $S_k^{\mathrm{edge}}(Z_k)$, $S_{j+1}^{\mathrm{left}}(X_j)$, or $S_k^{\mathrm{edge}}(Z_k')$, depending on a_0, completes the proof. It only remains to show that the commutations at each step of the algorithm are possible. Only the diagonal matrices $Z_k^{(i)}$ or $Z_k'^{(i)}$, are "moving" during the commutation, and these matrices commute with each other. So by (†), we just need to argue that, upon commuting $a = Z_k^{(i)}$, say, until it is adjacent to $a_0 = r(a)$, we do not need to commute $Z_k^{(i)}$ past any $X_{k-1}^{(i')}$. For concreteness, assume a_0 is of the form $X_k^{(i'')}$ with $i'' \leqslant i$. The argument is analogous in the cases where a_0 is of the form $X_k^{(i'')}$ with $i'' > i$, or $Z_k^{(1)}$ or $Z_k'^{(N-1)}$. The claim is clear when $i'' = i$, so assume $i'' < i$, so, in particular, $Z_k^{(i)}$ is being commuted to the left until it is just to the right of $X_k^{(i'')}$. Note such a $Z_k^{(i)}$ appears as a horizontal edge lying over the top of the small downward facing triangle corresponding to $X_k^{(i'')}$; compare with Figure 16. In the notation of Section 3.3.1, the horizontal segment $\mathrm{seg}(f(Z_k^{(i)})) \in \mathrm{Seg}_L$ in the discrete triangle Θ_{n-1} is of the form $\overline{(k, \beta, n-1-k-\beta)(k-1, \beta, n-k-\beta)}$. Thus the key observation is that if some snake-move matrix $M_{j_{i'}} = M_k$ contributes $X_{k-1}^{(i')}$ to M, then either the bottom snake $\sigma^{i'}$ of the i'–snake-move is later in the snake sequence than the bottom snake σ^i of the i–snake-move, in particular $i \leqslant i'$, or the top snake $\sigma^{i'+1}$ of the i'–snake-move is earlier in the snake sequence than the bottom snake $\sigma^{i''}$ of the i''–snake-move, in particular $i' + 1 \leqslant i''$. In the former case $X_{k-1}^{(i')}$ lies to the right of $Z_k^{(i)}$, and in the latter case $X_{k-1}^{(i')}$ lies to the left of $X_k^{(i'')}$. $\qquad \square$
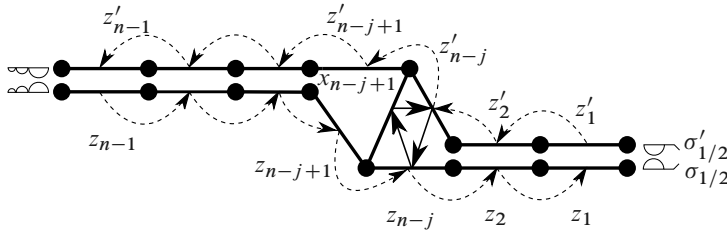
Figure 17: Right diamond snake-move algebra for $j = 2, \ldots, n-1$.
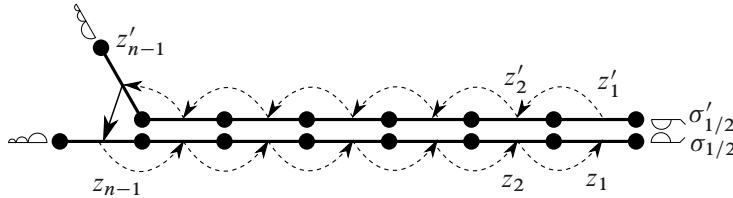
Figure 18: Right tail snake-move algebra for $j = 1$.

3.5 Setup for the quantum right matrix

We end with a few words about the proof for the quantum right matrix $\boldsymbol{M}_{\mathrm{FG}} = \boldsymbol{R}^\omega$, which essentially goes the same as for the left matrix.

(1) The right version of the jth snake algebra $\mathcal{S}_j^\omega$ for $j = 1, 2, \ldots, n-1$ is given by replacing the quivers of Figures 13 and 14 by the quivers shown in Figures 17 and 18.

(2) The jth quantum snake-move matrix $\boldsymbol{M}_j$ of Proposition 3.3 is replaced by

$$\boldsymbol{M}_j := \left[\left(\prod_{k=1}^{n-1} \boldsymbol{S}_k^{\text{edge}}(z_k) \right) \boldsymbol{S}_j^{\text{right}}(x_{n-j+1}) \left(\prod_{k=1}^{n-1} \boldsymbol{S}_k^{\text{edge}}(z_k') \right) \right] \in \mathrm{M}_n(\mathcal{S}_j^\omega).$$

Note, when $j = 1$, the matrix $\boldsymbol{S}_1^{\text{right}}(x_n) = \boldsymbol{S}_1^{\text{right}}$ is well defined, despite x_n not being defined.

(3) The subalgebra $\mathcal{T}_R \subseteq \mathcal{T}_n^\omega$ is generated by all but the $Z_j'^{\pm 1/n}$; see Figures 11 and 12.

Appendix Proof of Proposition 3.3

Lemma A.1 *If* $ZW = q^\epsilon WZ$ *in some quantum torus* $\mathcal{T}$, *and if* $\sum_{i=1}^m r_i = 0$, *then*

$$\prod_{i=1}^m [Z^{r_i} W^{r_i}] = 1 \in \mathcal{T}.$$

Proof Using $\left(\sum_i r_i \right)^2 / 2 = \sum_i r_i^2 / 2 + \sum_{i<j} r_i r_j$, we compute

$$\prod_i [Z^{r_i} W^{r_i}] = q^{-\epsilon \sum_i r_i^2 / 2} Z^{r_1} W^{r_1} Z^{r_2} W^{r_2} \cdots Z^{r_m} W^{r_m}$$

$$= q^{-\epsilon \sum_i r_i^2 / 2} q^{-\epsilon \sum_{i<j} r_i r_j} Z^{\sum_i r_i} W^{\sum_i r_i} = q^{-\epsilon (\sum_i r_i)^2 / 2} \cdot Z^0 \cdot W^0 = 1. \qquad \square$$

Proof of Proposition 3.3 As a shorthand, put $L_{il} := (S_j^{\text{left}}(x_{j-1}))_{il}$, $\widetilde{E}_{ii} := \prod_{k=1}^{n-1}(S_k^{\text{edge}}(z_k))_{ii}$, and $\widetilde{E}'_{ii} := \prod_{k=1}^{n-1}(S_k^{\text{edge}}(z'_k))_{ii}$. By Definition 2.6, and by the structure of the matrix $\boldsymbol{M}_j$, the following three relations are needed to establish that $\boldsymbol{M}_j$ is in $\text{M}_n^q(S_j^\omega)$:

(A-1) $[\widetilde{E}_{jj}L_{j(j+1)}\widetilde{E}'_{(j+1)(j+1)}][\widetilde{E}_{jj}L_{jj}\widetilde{E}'_{jj}] = q[\widetilde{E}_{jj}L_{jj}\widetilde{E}'_{jj}][\widetilde{E}_{jj}L_{j(j+1)}\widetilde{E}'_{(j+1)(j+1)}],$

(A-2) $[\widetilde{E}_{(j+1)(j+1)}L_{(j+1)(j+1)}\widetilde{E}'_{(j+1)(j+1)}][\widetilde{E}_{jj}L_{j(j+1)}\widetilde{E}'_{(j+1)(j+1)}]$

$$= q[\widetilde{E}_{jj}L_{j(j+1)}\widetilde{E}'_{(j+1)(j+1)}][\widetilde{E}_{(j+1)(j+1)}L_{(j+1)(j+1)}\widetilde{E}'_{(j+1)(j+1)}],$$

(A-3) $\qquad\qquad [\widetilde{E}_{ii}L_{ii}\widetilde{E}'_{ii}][\widetilde{E}_{kk}L_{kk}\widetilde{E}'_{kk}] = [\widetilde{E}_{kk}L_{kk}\widetilde{E}'_{kk}][\widetilde{E}_{ii}L_{ii}\widetilde{E}'_{ii}]$ for $i < k$.

We begin with (A-1). Note,

$$L_{j(j+1)} = L_{jj} = x_{j-1}^{(1-j)/n} \quad \text{and} \quad [\widetilde{E}_{jj}L_{j(j+1)}\widetilde{E}'_{(j+1)(j+1)}] = [\widetilde{E}_{jj}L_{jj}\widetilde{E}'_{jj}z_j'^{-1}].$$

So it suffices to show that commuting $z_j'^{-1}$ from left to right across $\widetilde{E}_{jj}L_{jj}\widetilde{E}'_{jj}$ contributes a factor q, equivalently, z'_j contributes q^{-1}. Indeed, in $\widetilde{E}_{jj}L_{jj}\widetilde{E}'_{jj}$ we see z'_j only interacts with $x_{j-1}^{(1-j)/n}$ with weight q^2, with $(S_j^{\text{edge}}(z_j))_{jj} = z_j^{(n-j)/n}$ with weight q^{-2}, with $(S_{j+1}^{\text{edge}}(z'_{j+1}))_{jj} = z_{j+1}'^{(n-j-1)/n}$ with weight q, and with $(S_{j-1}^{\text{edge}}(z'_{j-1}))_{jj} = z_{j-1}'^{(1-j)/n}$ with weight q^{-1}. The total exponent of q that z'_j contributes is therefore $(2(1-j) - 2(n-j) + 1(n-j-1) - 1(1-j))/n = -1$.

Next we check (A-2). Note, $L_{(j+1)(j+1)} = L_{j(j+1)} = x_{j-1}^{(1-j)/n}$ and $[\widetilde{E}_{jj}L_{j(j+1)}\widetilde{E}'_{(j+1)(j+1)}] = [z_j\widetilde{E}_{(j+1)(j+1)}L_{(j+1)(j+1)}\widetilde{E}'_{(j+1)(j+1)}]$. So it suffices to show that commuting z_j from right to left across $\widetilde{E}_{(j+1)(j+1)}L_{(j+1)(j+1)}\widetilde{E}'_{(j+1)(j+1)}$ contributes a factor q. Indeed, in

$$\widetilde{E}_{(j+1)(j+1)}L_{(j+1)(j+1)}\widetilde{E}'_{(j+1)(j+1)}$$

we see that z_j only interacts with $x_{j-1}^{(1-j)/n}$ with weight q^2 (because it's moving from right to left), with $(S_j^{\text{edge}}(z'_j))_{(j+1)(j+1)} = z_j'^{-j/n}$ with weight q^{-2}, with $(S_{j+1}^{\text{edge}}(z_{j+1}))_{(j+1)(j+1)} = z_{j+1}^{(n-j-1)/n}$ with weight q, and with $(S_{j-1}^{\text{edge}}(z_{j-1}))_{(j+1)(j+1)} = z_{j-1}^{(1-j)/n}$ with weight q^{-1}. The total exponent of q that z_j contributes is therefore $(2(1-j) - 2(-j) + 1(n-j-1) - 1(1-j))/n = +1$.

Lastly we verify (A-3). Note that the terms in $[\widetilde{E}_{ii}L_{ii}\widetilde{E}'_{ii}]$ appear in the forms $x_{j-1}^{\alpha^i}$ or $z_l^{\beta_l^i}z_l'^{\beta_l^i}$ for $l = 1, 2, \ldots, n-1$. We see from the quivers in Figures 13 and 14 that terms of this form mutually commute. So

$$[\widetilde{E}_{ii}L_{ii}\widetilde{E}'_{ii}] = [x_{j-1}^{\alpha^i}]\prod_l[z_l^{\beta_l^i}z_l'^{\beta_l^i}],$$

where the right-hand side is independent of the ordering of the terms. Similarly for $[\widetilde{E}_{kk}L_{kk}\widetilde{E}'_{kk}]$. It follows that $[\widetilde{E}_{ii}L_{ii}\widetilde{E}'_{ii}]$ commutes with $[\widetilde{E}_{kk}L_{kk}\widetilde{E}'_{kk}]$ for all i and k.

It remains to check that the quantum determinant of $\boldsymbol{M}_j$ is equal to $1 \in S_j^\omega$. Since $\boldsymbol{M}_j$ is in $\text{M}_n^q(S_j^\omega)$ and is triangular, by Remark 2.7(1) we have $\text{Det}^q(\boldsymbol{M}_j) = \prod_i(\boldsymbol{M}_j)_{ii}$. As the only l such that z_l does not commute with z'_l is $l = j$, the above equation becomes

$$(\boldsymbol{M}_j)_{ii} = [\widetilde{E}_{ii}L_{ii}\widetilde{E}'_{ii}] = [z_j^{\beta_j^i}z_j'^{\beta_j^i}]x_{j-1}^{\alpha^i}\prod_{l \neq j}(z_lz_l')^{\beta_l^i}.$$

Note, $\sum_i \alpha^i = 0$ and $\sum_i \beta_l^i = 0$ for all $l = 1, 2, \ldots, n-1$ by construction of $\boldsymbol{M}_j$ (this is where the normalizing factors come in; compare with the example below Proposition 3.3). It follows that (where the last equality is by Lemma A.1),

$$\mathrm{Det}^q(\boldsymbol{M}_j) = \left(\prod_i [z_j^{\beta_j^i} \, 'z_j^{\beta_j^i}]\right) \left(\prod_i x_{j-1}^{\alpha^i} \prod_{l \neq j} (z_l z_l')^{\beta_l^i}\right) = \left(\prod_i [z_j^{\beta_j^i} \, 'z_j^{\beta_j^i}]\right) 1 = 1. \qquad \square$$

References

[1] **F Bonahon**, **H Wong**, *Quantum traces for representations of surface groups in* $\mathrm{SL}_2(\mathbb{C})$, Geom. Topol. 15 (2011) 1569–1615 MR Zbl

[2] **K A Brown**, **K R Goodearl**, *Lectures on algebraic quantum groups*, Birkhäuser, Basel (2002) MR Zbl

[3] **D Bullock**, **C Frohman**, **J Kania-Bartoszyńska**, *Understanding the Kauffman bracket skein module*, J. Knot Theory Ramifications 8 (1999) 265–277 MR Zbl

[4] **L O Chekhov**, **M Shapiro**, *Log-canonical coordinates for symplectic groupoid and cluster algebras*, Int. Math. Res. Not. 2023 (2023) 9565–9652 MR Zbl

[5] **D C Douglas**, *Classical and quantum traces coming from* $\mathrm{SL}_n(\mathbb{C})$ *and* $\mathrm{U}_q(\mathfrak{sl}_n)$, PhD thesis, University of Southern California (2020) Available at https://www.proquest.com/docview/2436891478

[6] **D C Douglas**, *Quantum traces for* $\mathrm{SL}_n(\mathbb{C})$: *The case* $n = 3$, J. Pure Appl. Algebra 228 (2024) art. id. 107652 MR Zbl

[7] **V V Fock**, **L O Chekhov**, *Quantum Teichmüller spaces*, Teoret. Mat. Fiz. 120 (1999) 511–528 MR Zbl In Russian; translated in Theoret. and Math. Phys. 120 (1999) 1245–1259

[8] **V V Fock**, **A B Goncharov**, *Cluster* $\mathcal{X}$*–varieties, amalgamation, and Poisson–Lie groups*, from "Algebraic geometry and number theory" (V Ginzburg, editor), Progr. Math. 253, Birkhäuser, Boston, MA (2006) 27–68 MR Zbl

[9] **V V Fock**, **A B Goncharov**, *Moduli spaces of local systems and higher Teichmüller theory*, Publ. Math. Inst. Hautes Études Sci. 103 (2006) 1–211 MR Zbl

[10] **V V Fock**, **A B Goncharov**, *Dual Teichmüller and lamination spaces*, from "Handbook of Teichmüller theory, I" (A Papadopoulos, editor), IRMA Lect. Math. Theor. Phys. 11, Eur. Math. Soc., Zürich (2007) 647–684 MR Zbl

[11] **V V Fock**, **A B Goncharov**, *Moduli spaces of convex projective structures on surfaces*, Adv. Math. 208 (2007) 249–273 MR Zbl

[12] **V V Fock**, **A B Goncharov**, *Cluster ensembles, quantization and the dilogarithm*, Ann. Sci. Éc. Norm. Supér. 42 (2009) 865–930 MR Zbl

[13] **D Gaiotto**, **G W Moore**, **A Neitzke**, *Spectral networks and snakes*, Ann. Henri Poincaré 15 (2014) 61–141 MR Zbl

[14] **M Gekhtman**, **M Shapiro**, **A Vainshtein**, *Poisson geometry of directed networks in a disk*, Selecta Math. 15 (2009) 61–103 MR Zbl

[15] **W M Goldman**, *The symplectic nature of fundamental groups of surfaces*, Adv. in Math. 54 (1984) 200–225 MR Zbl

[16] **W M Goldman**, *Invariant functions on Lie groups and Hamiltonian flows of surface group representations*, Invent. Math. 85 (1986) 263–302 MR Zbl

[17] **A Goncharov**, **L Shen**, *Quantum geometry of moduli spaces of local systems and representation theory*, preprint (2019) arXiv 1904.10491

[18] **N J Hitchin**, *Lie groups and Teichmüller space*, Topology 31 (1992) 449–473 MR Zbl

[19] **L Hollands**, **A Neitzke**, *Spectral networks and Fenchel–Nielsen coordinates*, Lett. Math. Phys. 106 (2016) 811–877 MR Zbl

[20] **R M Kashaev**, *Quantization of Teichmüller spaces and the quantum dilogarithm*, Lett. Math. Phys. 43 (1998) 105–115 MR Zbl

[21] **C Kassel**, *Quantum groups*, Graduate Texts in Math. 155, Springer (1995) MR Zbl

[22] **G Kuperberg**, *Spiders for rank 2 Lie algebras*, Comm. Math. Phys. 180 (1996) 109–151 MR Zbl

[23] **F Labourie**, *Anosov flows, surface groups and curves in projective space*, Invent. Math. 165 (2006) 51–114 MR Zbl

[24] **G Martone**, *Positive configurations of flags in a building and limits of positive representations*, Math. Z. 293 (2019) 1337–1368 MR Zbl

[25] **D Mumford**, **J Fogarty**, **F Kirwan**, *Geometric invariant theory*, 3rd edition, Ergebnisse der Math. 34, Springer (1994) MR Zbl

[26] **C Procesi**, *The invariant theory of $n \times n$ matrices*, Advances in Math. 19 (1976) 306–381 MR Zbl

[27] **J H Przytycki**, *Skein modules of 3–manifolds*, Bull. Polish Acad. Sci. Math. 39 (1991) 91–100 MR Zbl

[28] **G Schrader**, **A Shapiro**, *Continuous tensor categories from quantum groups*, *I*: *Algebraic aspects*, preprint (2017) arXiv 1708.08107

[29] **G Schrader**, **A Shapiro**, *A cluster realization of $U_q(\mathfrak{sl}_n)$ from quantum character varieties*, Invent. Math. 216 (2019) 799–846 MR Zbl

[30] **A S Sikora**, *Skein theory for $\mathrm{SU}(n)$–quantum invariants*, Algebr. Geom. Topol. 5 (2005) 865–897 MR Zbl

[31] **W P Thurston**, *Three-dimensional geometry and topology, 1*, Princeton Mathematical Series 35, Princeton Univ. Press (1997) MR Zbl

[32] **V G Turaev**, *Algebras of loops on surfaces, algebras of knots, and quantization*, from "Braid group, knot theory and statistical mechanics" (C N Yang, M L Ge, editors), Adv. Ser. Math. Phys. 9, World Sci., Teaneck, NJ (1989) 59–95 MR Zbl

[33] **E Witten**, *Quantum field theory and the Jones polynomial*, Comm. Math. Phys. 121 (1989) 351–399 MR Zbl

Department of Mathematics, Virginia Tech
Blacksburg, VA, United States

dcdouglas@vt.edu

ALGEBRAIC & GEOMETRIC TOPOLOGY